Physiol Rev 85: 943–978, 2005;
doi:10.1152/physrev.00020.2004.

Controlling Cell Behavior Electrically: Current Views and Future Potential

COLIN D. McCAIG, ANN M. RAJNICEK, BING SONG, AND MIN ZHAO

School of Medical Sciences, Institute of Medical Sciences, University of Aberdeen, Aberdeen, Scotland

McCaig, Colin D., Ann M. Rajnicek, Bing Song, and Min Zhao. Controlling Cell Behavior Electrically: Current Views and Future Potential. *Physiol Rev* 85: 943-978, 2005; doi:10.1152/physrev.00020.2004.—Direct-current (DC) electric fields are present in all developing and regenerating animal tissues, yet their existence and potential impact on tissue repair and development are largely ignored. This is primarily due to ignorance of the phenomenon by most researchers, some technically poor early studies of the effects of applied fields on cells, and widespread misunderstanding of the fundamental concepts that underlie bioelectricity. This review aims to resolve these issues by describing: *1*) the historical context of bioelectricity, *2*) the fundamental principles of physics and physiology responsible for DC electric fields within cells and tissues, *3*) the cellular mechanisms for the effects of small electric fields on cell behavior, and *4*) the clinical potential for electric field treatment of damaged tissues such as epithelia and the nervous system.

I. INTRODUCTION

This review discusses the existence of DC electrical gradients of voltage within tissues (endogenous electrical fields), how cells respond to these gradients, and their role in development and in tissue repair. Because these steady, extracellular voltage gradients differ from the type of fast, transmembrane-associated electrical events familiar to present-day electrophysiologists, we open with a historical background that traces their parallel origins and highlights mechanistic similarities and differences.

II. HISTORICAL BACKGROUND

A. The Common Origins of Electrophysiology and Bioelectricity

In the mid-1700s, the ability to store and discharge static electricity from a Leyden jar was discovered and was used to demonstrate the effects of delivering strong electrical shocks to people. Vanable (198), quoting Hoff (79), recounts that L'Abbe Jean-Antoine Nollet caused 180 of the King's guards to leap simultaneously by having them all hold hands and then connecting the man at the

end of the line to the discharge from a Leyden jar. The King was greatly amused! This public party-trick was repeated with the whole population of a Carthusian monastery, which strung out a mile's worth of humanity that leaped in concert on receiving the charge.

Around the same time, the importance of the electrical control of cell physiology was becoming apparent from the famous experiments of Galvani (Fig. 1A) (70, 159, 160). His epic work on frog nerve-muscle preparations included the use of lightning rods connected to nerves via wires, which caused leg muscles to twitch during a lightning storm. Similarly, static electricity generators creating sparks that activated nerve conduction also caused muscle twitching. Equally important was his observation during a public experiment in Bologna in 1794 that the cut end of a frog sciatic nerve from one leg stimulated contractions when it touched the muscles of the opposite leg. Collectively, these experiments provided definitive evidence for "animal electricity." In addition, with this last experiment, Galvani had demonstrated the existence of the injury potential (Fig. 1*A*).

1. Injury potentials and action potentials

An injury potential is a steady, long-lasting direct-current (DC) voltage gradient induced within the extracellular and intracellular spaces by current flowing into and around an injured nerve. Its discovery predated the discovery of the better known action potential, which is a rapid, self-regenerating voltage change localized across the cell membrane. In 1831, Matteucci extended Galvani's observations by measuring injury potentials directly at the cut end of nerves and muscles using a galvanometer (named after Galvani). Ingeniously, he used the injury potential of damaged frog muscle to demonstrate the existence of action potentials in nerve and muscle for the first time. By placing a cut nerve into an injured muscle (Fig. 1*A*), he showed that the latter activated the nerve and caused contraction of the muscle innervated by that nerve. He showed also that muscles made to contract in this way would activate contractions in a second frog muscle preparation, whose intact nerves were placed across the belly of the twitching muscles. The action potentials of the uninjured muscle fibers had stimulated action potentials in the intact nerves and intact muscles of the second preparation. In the intervening two centuries, the relative importance of injury potentials and action potentials has shifted markedly. Action potentials are central in neuroscience and electrophysiology, but injury potentials are frequently not recognized, are neglected, or are grossly misunderstood.

2. Injury potentials and nerve regeneration

Part of this review will discuss the role of endogenous and applied electrical fields (EFs) in stimulating and directing nerve growth and nerve regeneration. It is important and instructive to draw a clear historical link. Recent work in this area begins with experiments that are direct descendants of Galvani's work on injury potentials. Injury currents, like those discovered by Galvani, have been measured entering the cut ends of Mauthner and Muller axons in embryonic lamprey spinal cord (Fig. 1*B*) (22). These currents are of the order of 100 μA/cm^2, and because the resistivity of soft tissues is ~1,000 $\Omega \cdot$ cm, they give rise to steady voltage gradients of ~10 mV/mm. The hypothesis that the injury potential these currents establish in the distal ends of cut axons might impede regeneration has been tested. So has the proposal that applying a DC EF to offset and reverse the polarity of this injury potential would promote regeneration (24). Both have proven correct. In the intervening 20 years, this work has progressed to human clinical trials using applied DC EFs to treat human spinal cord injuries (see sect. VI).

3. Injury potentials and wound healing

The great German physiologist Emil Du-Bois Reymond, considered to be the founder of modern electrophysiology, repeated Matteucci's experiments and measured directly the propagating action potential. However, he was also interested in injury potentials. In 1843, he used a galvanometer (built with >2 miles of wire) to measure ~1 μA flowing out of a cut in his own finger. The flow of current is due to the short-circuiting of the transepithelial potential (TEP) difference that occurs at a skin lesion (Fig. 1, *C–F*).

A second aspect of this review discusses the role of endogenous and applied EFs in stimulating and directing wound healing. Again, a direct historical link is appropriate. Recent work in this area begins with two studies that are clear descendants of Du-Bois Reymond's demonstration of injury currents in skin. First, the stumps of regenerating newt limbs drive large currents out the cut end (29). Currents of between 10 and 100 μA/cm^2 create a steady voltage drop of ~60 mV/mm within the first 125 μm of extracellular space, and this is essential for regeneration (2, 95, 133, 134). Second, human skin and that of guinea pigs and amphibians maintain a TEP across the epithelial layers. When the skin is cut, a large, steady EF arises immediately and persists for hours at the wound edge, as current pours out the lesion from underneath the wounded epithelium (Fig. 1, *D* and *F*) (8). These fields measure ~140 mV/mm and play important roles in controlling several aspects of the cell biology of wound healing (see sect. V*D*).

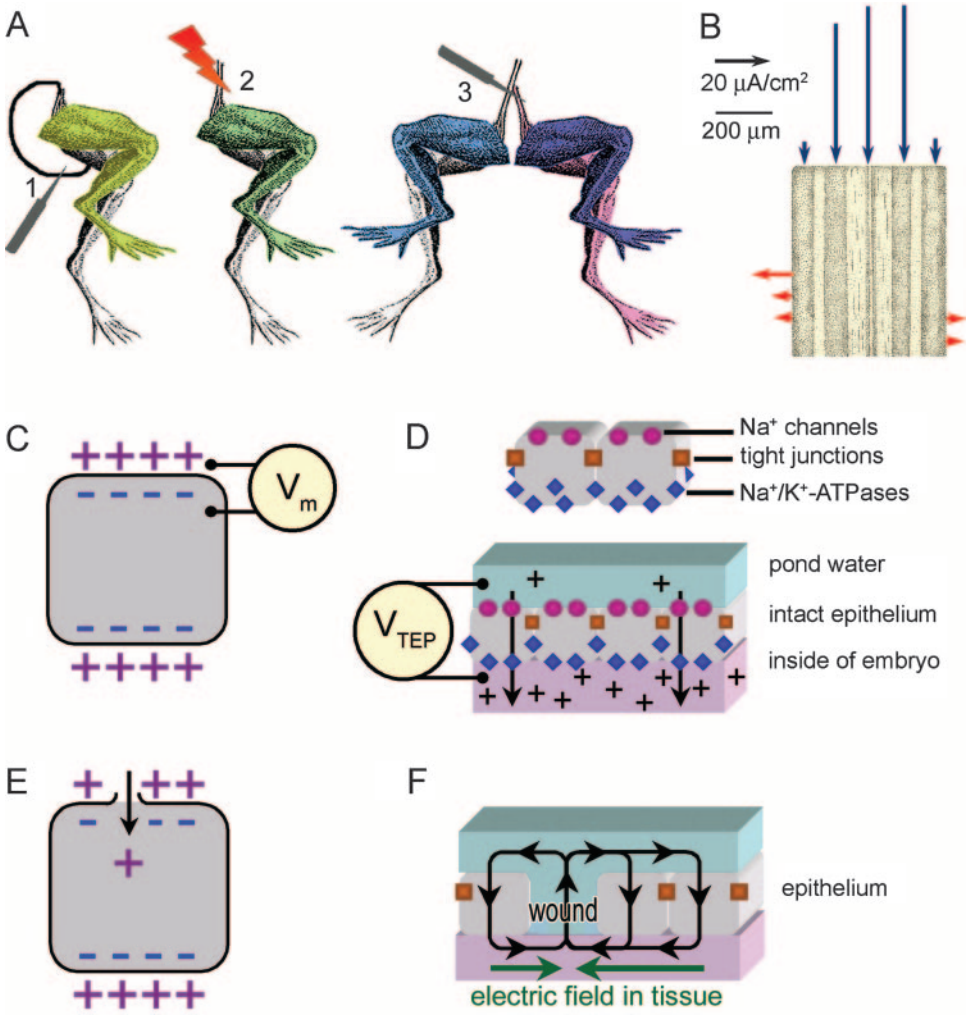

FIG. 1. The historical context, concepts of bioelectricity, and the injury potential. *A*: Galvani's 18th century experiments using a frog leg preparation. The leg contracted when the cut end of the sciatic nerve touched the leg muscle (*1*) or when the electrical discharge from a Leyden jar was applied directly to the nerve (*2*). When the surface of a section of the right sciatic nerve touched the intact surface of the left sciatic nerve, both legs contracted (*3*). He concluded that electrical conduction ("animal electricity") was required for muscle contraction, but it wasn't until the 19th century that Mateucci's measurements showed that the source of "animal electricity" was the potential difference between injured and intact surfaces, the injury potential. *B*: 20th century parallels with Galvani's studies revealed injury currents entering the cut ends of axons in the lamprey spinal cord. A sensitive, rapidly vibrating, voltage-sensing electrode (see Fig. 4*D*) was placed near the cut surface of the spinal cord (*top*). The blue arrows pointing down indicate an injury current entering the cut ends of axons. The red arrows at the sides of the cord indicate a region of outward current. By convention the direction of current flow is taken to be the direction of the flow of positively charged ions. [Modified from Borgens et al. (22).] *C*: individual cells maintain an electrical potential (V_m) across the intact plasma membrane. This results from the activity of membrane-bound channels selective for transport of specific ions across the intact membrane, which has a high electrical resistance. The result is a net negative charge on the inside of the cell relative to the outside. *D*: similarly, selective, directional ion transport across intact epithelia results in a significant potential difference across the epithelial layer. Embryonic *Xenopus* skin is used in this example, but the principles apply to all ion-transporting epithelia, including multilayered epithelia, such as mammalian skin and the corneal epithelium. *Xenopus* skin scavenges Na^+ from the dilute pond water in which it is bathed via the spatial separation of Na^+ channels and pumps within epithelial cell membranes. Each cell is divided functionally into an apical domain facing the pond water and a basolateral domain facing the inside of the embryo. The apical domain contains membrane proteins that allow passive entry of Na^+ (arrow) into the cell, and the basolateral domain contains Na^+-K^+-ATPases that actively pump Na^+ out of the cell into the intercellular embryonic space (arrow). Tight junctions between epithelial cells provide physical connections between cells, providing high electrical resistance to the epithelial sheet and preventing leakage of Na^+ out of the embryo. The result is a higher concentration of Na^+ inside the skin relative to the outside. The resulting transepithelial potential (TEP) gradient of tens of millivolts can be measured directly across the intact epithelium. Intact skin therefore represents a biological "battery." *E*: in an individual cell, localized injury to the membrane causes an inward injury current as positively charged ions enter the cytoplasm. This underlies the inward currents measured at the cut axons in the lamprey spinal cord (see *B*) and other cells. *F*: wounding of an epithelial sheet (or localized disruption of tight junctions) creates a current leak at the wound site causing the immediate, catastrophic collapse of the TEP at the wound. The TEP is not affected distally however, where the epithelial integrity and ion transport properties remain intact. Na^+ leak out the wound, resulting in an outward injury current and a lateral voltage gradient (electric field) within the embryo (green arrows) oriented parallel to the epithelial sheet. The wound site is the cathode of the electric field.

Interestingly, although frog nerve and frog skin were key preparations in the discovery of steady DC injury potentials and have been central to teaching in electrophysiology, it is for the action potential and the TEP that these tissues are best known. Few of the many pupils and teachers that have used these preparations are familiar with injury potentials or their essential role in tissue development and repair.

In parallel with Galvani's work, Volta was developing these ideas to create the first battery. Recognizing the parallel with animal electricity, Volta used batteries therapeutically to treat deafness. Others, however, were less rigorous scientifically in the promotion of electrical-based therapies. For more than a century there was "widespread and irrational use of galvanism and static electricity" (198). Static electricity generators were in common use and were promoted and sold because they created an allegedly beneficial "electric air bath" or a "negative breeze." The electric air bath involved charging the patient and using a grounded electrode to draw sparks from a chosen part of the body. The negative breeze allegedly was helpful in treating insomnia, migraine, and baldness (Fig. 2). With the electrode polarity reversed, a "positive breeze" was used to treat kidney disease. Vanable (198) gives a good account of this charlatanism and makes the insightful point that this period of highly dubious pseudoscience tainted perceptions and may be a major reason why animal electricity and bioelectricity have been held in relatively low scientific esteem.

FIG. 2. An electric air bath ("negative breeze"). The wooden cabinet houses a static electricity generator that is connected to a metal plate under the patient's feet. A metal cathode suspended above the patient's head completes the circuit. This therapy was used in the 19th century to treat conditions such as insomnia, baldness, migraine, and early kidney disease. When treatment with "negative breeze" therapy was unsuccessful, the electrodes were sometimes reversed and "positive breeze" therapy was applied. By the 20th century, such treatment was dismissed as "quackery" due to an improved understanding of the cellular physiology underpinning the electrical component of tissue repair and development. [Modified from Borgens (16).]

This historical preamble is relevant for two reasons. First, by describing the pioneering work on animal electricity and bioelectricity, we make the point that these phenomena share a common foundation in elemental electrophysiology, yet the latter enjoys far greater scientific respectability. Second, it shows that from its inception even in mainstream physiology, there were elements of awe, wonder, and showmanship in the study of bioelectricity. Moreover, because some of this background work has involved outright quackery, there is a danger that we dismiss all of it. One aim of this review will be to restore scientific credibility to neglected aspects of animal electricity. This is a realistic aim because these concepts have a real basis in physiology and because they can (and do) sit comfortably beside the fast, channel-centered, membrane electrophysiology of the present day. These concepts are summarized in Figure 1.

B. Electrical Signals Vary in Space and Time

Contemporary electrophysiologists are familiar with fast membrane conductance changes that take place within milliseconds, for example, as an action potential is propagated along a neuronal membrane. In developmental biology too there is widespread recognition of similarly fast electrical conductance changes, for example, across the egg membrane. In this case, a transient and massive membrane depolarization of the newly fertilized sea urchin egg acts as an electrical block to polyspermy (87). Both of these examples involve very fast conductance changes that occur within membrane-embedded channels and a flow of ions that changes the voltage across the membrane only. The electrical events to be covered in this review last much longer and are present across hundreds of microns, rather than being confined to the immediate vicinity of the cell membrane. They involve steady DC gradients of electrical potential, usually in the extracellular spaces, but sometimes within the cytoplasm of a single cell or a syncytium of cells. Such gradients are present for hours, days, or even weeks during both development and regeneration. In addition, they are regulated both spatially and developmentally. Their undisputed existence and their physiological relevance, both of which will be established below, indicate that they should be integrated into current thinking. One way to do this is to consider throughout this review the issue of chemotaxis. This is a widely accepted form of directed cell motility based on the ability of cells to respond with directional movement in a chemical gradient. Many types of mole-

cules are presented to cells in the form of chemical gradients in the extracellular spaces. Both in developing and in regenerating systems many of these molecules carry a net charge. Because steady voltage gradients also are present within the extracellular spaces and vary in space and time, these coexistent chemical and electrical signals must interact. This raises several issues. For example, are chemical gradients established by preexisting electrical gradients? Do chemical and electrical guidance cues activate shared signaling pathways to achieve directional growth? Are there hierarchies of guidance cues that vary in space and time?

Some other questions to be tackled are outlined below, to prime the reader. As the review develops, the answers to these questions will need to be integrated with prevailing views on the control of directed cell motility by chemical gradients (177), or by substrate topography (147), or by whatever other dynamic guidance cues coexist within the extracellular spaces. Where are steady electrical fields found? What is their basis? What are their functions? What tissue or cellular effects do they have? What mechanisms underpin these effects? How do electrical cues interact with other guidance cues? And can electrical fields be mimicked or manipulated to control cell behaviors?

III. FUNDAMENTAL CONCEPTS IN ELECTROPHYSIOLOGY

Understanding the origins and interdependence of steady DC currents and associated voltage gradients is central to all that follows. Although this involves nothing more complex than Ohm's law, the unfamiliarity of these concepts to some biologists makes it appropriate to revisit high school physics. This has been covered thoroughly in a fine review by Robinson and Messerli (173). One of the simplest of electrical circuits is formed by a resistor connected to the two terminals of a voltage source, or battery, by conducting wires (Fig. 3*A*). Current is carried in the wires by electrons, and there is a direct relationship between the voltage difference across the resistor and the current that flows through it. This is known as Ohm's law : $V = I \cdot R$, where V is the voltage of the battery, I is the current (in amps), and R is the resistance (in ohms). In a physiological solution such as the cytoplasm or the fluids of the extracellular spaces, there are no free electrons to carry charge so current is carried by charged ions such as Na^+ and Cl^- instead. The bulk resistivity of a physiological solution can be measured and typically is ~100 $\Omega \cdot$ cm. If there is a voltage difference between any two points in a conductive medium, current will flow. The voltage difference per unit distance is the electrical field, and in a biological context, this is most intuitively expressed in millivolts per millimeter. The relationship between current density and the electrical field is $E = J \cdot \rho$, where E is the electrical field, J is the current density (in A/cm^2), and ρ is the resistivity of the medium. Inevitably then the existence of an EF and the flow of current are interdependent and inseparable events. Importantly, the EF and the current density are vectors, with both magnitude and direction. It is this directional quality of an EF that makes it a candidate spatial organizer, because it can impose directional movement on chemicals in the extracellular environment, on receptor molecules, on cells, and on tissues.

In addition to acting as a vector, current flow and voltage gradients in tissues also vary in space and time. This happens for two reasons: *1*) functional ion channels

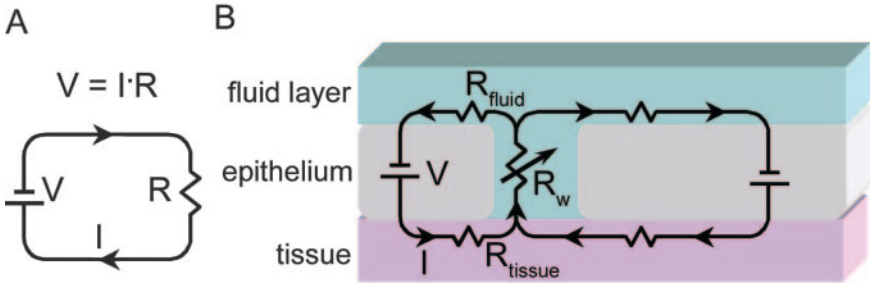

FIG. 3. Electrical properties of wounded epithelia and surrounding tissue. *A*: a simple, nonbiological electric circuit. Wires connect a battery (V) to a resistor (R). Electrons, which are negatively charged, carry the current (I, arrows) within the wire. The relationship between the voltage difference across the resistor and the current flowing through it is described by Ohm's law: $V = IR$. *B*: in an ion-transporting epithelium, the transepithelial potential difference (TEP) of several tens of millivolts (Fig. 1*D*) acts as a "skin battery" (V). In biological systems the current (I) is carried by charged ions, such as Na^+ and Cl^-. Injury to the epithelium produces a low resistance path by which ions leak out through the wound. The resistance of the wound (R_w) is variable; R_w is higher if the wound is allowed to dry out than if the wound has a moist dressing. In frog skin and corneal epithelium, in which the outer layer of the epithelium is constantly bathed in a conductive fluid, the resistance of the return path of the current (R_{fluid}) is low compared with that within the tissue (R_{tissue}). As a result, most of the lateral potential drop is within the subepidermal tissue layer; therefore, a lateral electric field exists in the region near the wound. Because the direction of current flow is taken to be the direction of flow of positive ions (arrows), the wound is more negative than distal regions within the tissue. The wound therefore represents the cathode of the naturally occurring subepidermal electric field.

and/or ion pumps may be localized to separate cells, or parts of cells, and this pattern of localization/activation may change with time; and *2*) the local resistance of a tissue may vary as a consequence of wounding, which creates holes (current leaks, Fig. 3*B*), spatial variation in cell packing, or transient breakdown of tight junctions to permit cell movements. Two examples of the latter come from regenerating and developing limbs. Stump currents associated with amputation of the urodele limb have been mentioned already; 10–100 μA/cm^2 leave the stump and in the first hours after injury create a DC voltage drop of ~60 mV/mm within 125 μm of the lesion. By 6 h postlesion as the stump wound resistance increases, the EF drops to 26 mV/mm, distally negative (133, 134). Second in development, the tight junctions between epithelial cells of the flank skin break down, but only in the precise areas where limb buds will form. The TEP becomes short-circuited only at these sites from which currents of 1–10 μA/cm^2 leave the flank. These "prophetic" currents precede limb bud emergence by several days and predict the sites from which limb buds will appear in amphibians, chicks, and mice (1, 21, 25, 170).

Before discussing more detailed examples of electrical fields and their control of development and regeneration, it is crucial to put the magnitude of these electrical signals into context. To depolarize a neuron and fire an action potential using surface electrodes requires field stimulation of 1–2 V/mm. The common technique of electroporation for drug or gene delivery into cells uses extremely large pulses of DC EF stimulation, roughly 100–500 V/mm (143). The DC EFs that play physiological roles in development and regeneration (see examples in sect. IV, *A–D*) are three or four orders of magnitude less than this (1–100 mV/mm)! It is a mistake to think of them having similar magnitude, but this is a major misconception made by those who dismiss EF as being "nonphysiological."

IV. ELECTRICAL FIELDS EXIST EXTRACELLULARLY AND INTRACELLULARLY

Four biological examples follow that put these concepts into context. The first two generate an image of dynamic electrical signals present within the extracellular spaces as potential guidance cues for migrating or proliferating cells. The latter two show that steady electrical signals also exist across contiguous cytoplasmic regions within and between some cells; for example, those coupled by gap junctions.

A. Example 1: Embryos Generate a Dynamic Voltage Gradient Across Their Skin

The skin of adult frogs is well known as a transporting epithelium that sustains a TEP of ~100 mV, inside positive, across the multilayered epithelium (102). The ion transport properties of the apical and basolateral cell membranes differ and are polarized (Fig. 1*D*). The apical cell membrane contains specialized amiloride-sensitive sodium channels allowing Na^+ to enter the cells, while the basolateral membranes contain the well-known "sodium pump," the ouabain-sensitive Na^+-K^+-ATPase that electrogenically pumps three Na^+ from the cytoplasm out into the extracellular fluid in exchange for two K^+ entering the cells. Net ion transport therefore occurs across the epithelium, with Na^+ being transported from pond water into the animal. A high-resistance electrical "seal" exists between neighboring cells in most epithelial sheets including amphibian skin. This is formed by tight junctions, and these greatly reduce the electrical conductivity of the paracellular space (5). Viewed end-on, the apical surface of each epithelial cell appears to be encircled by strands of specialized tight junctional proteins. Strands on neighboring cells abut each other to form a "seal" that restricts the paracellular passage of solutes and water. The whole structure may be pictured as similar to a series of interconnecting hoops around the end of a barrel. The same basic elements of polarized channels, pumps, and tight junctions are found in embryonic frog skin, and these also establish a TEP from very early stages of development (131, 168).

1. Voltage gradients exist within the extracellular spaces underneath the skin

Crucially, the potential difference across the skin is different in different parts of the developing embryo (180). With the use of standard glass microelectrodes, stable gradients of voltage have been measured around the neural plate area in axolotl embryos during the period of neurulation. Skin potentials are higher rostrally than caudally (Fig. 4, *A–C*). This is particularly marked at the head end of the embryo, where EFs of 75–100 mV/mm have been measured in the extracellular space below the epithelium (180), whilst EFs of 30 mV/mm are present in the region rostral to the developing blastopore (173). In both cases the orientation of the steady voltage gradient is rostrocaudal, that is, along the long axis of the embryo (head to tail). The skin potential also is high at the midline of the neural plate as it begins to fold over to become the neural tube, decreases at the neural folds, and increases again further laterally on the flank of the embryo. This pattern of skin potential gives rise to standing voltage gradients on either side of the dorsal midline, with a mediolateral orientation (Fig. 4, *A–C*).

The point was made above that voltage gradients and current flow are linked inextricably, and these findings of voltage gradients using glass microelectrodes impaling the skin have been paralleled using a second, less familiar technique that measures current flow noninvasively

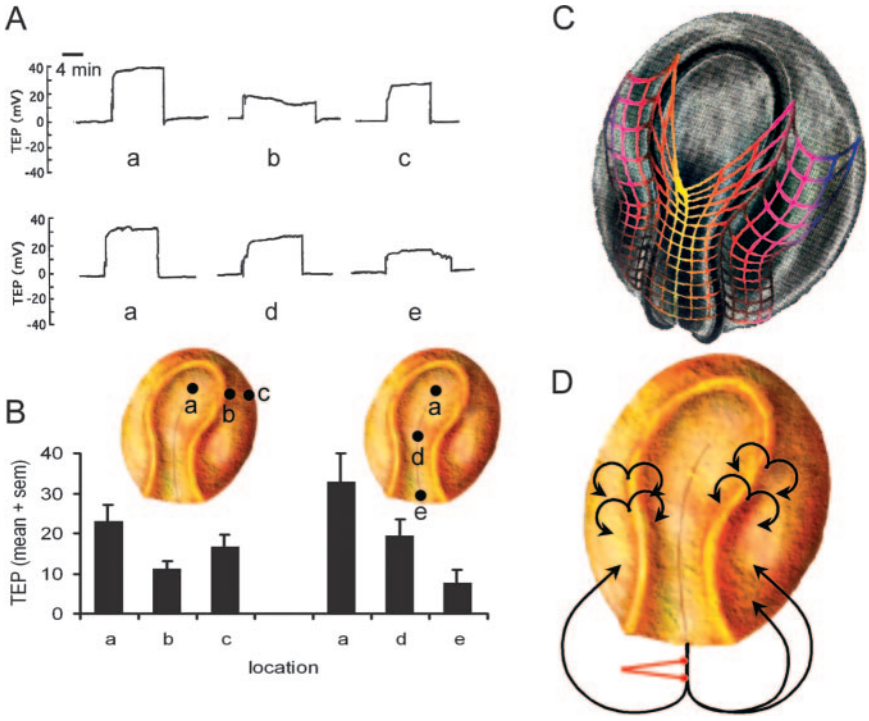

FIG. 4. Spatial differences in the transepithelial potential difference (TEP) generate electric fields within intact embryos. *A*: TEP measurements made using glass voltage-sensing electrodes. The TEP of axolotl embryos was measured relative to a bath ground electrode at the time of early neural tube formation (stage 16) in three positions on the same embryo. Measurement sites are shown in *B*: *a*, at the rostral end of the neural groove; *b*, at the lateral edge of the neural fold; *c*, at the lateral epithelium; *d*, halfway along the neural groove; *e*, at the caudal end of the neural groove near the blastopore. The TEP at each site was positive on the inside of the embryo. [Data from Shi and Borgens (180).] *B*: TEP measurements made at sites *a*, *b*, and *c* in 8 embryos demonstrating that the TEP is highest in the center of the neural groove (*a*) and lowest at the lateral edge of the neural ridge (*b*). Measurements from 20 embryos at sites *a*, *d*, and *e* indicate a rostral to caudal TEP gradient. [Data from Shi and Borgens (180); embryo in *B* and *D* modified from Borgens and Shi (26).] *C*: an artist's impression of the spatial differences of TEP in a stage 16 axolotl embryo. Colors represent the magnitude of the TEP. Yellow is highest, and purple is lowest. The slope of the line indicates the magnitude of the resulting local electric field in the subepidermal tissues. [Modified from Shi and Borgens (180).] *D*: current loops detected using a noninvasive vibrating electrode. The electrode vibrates rapidly near the embryo in an electrically conductive medium (e.g., pond water). The stainless steel electrode has a small voltage-sensing platinum ball at its tip, which is vibrated rapidly over a distance of ~20 μm. The electrode (red) is shown at the extremes of its vibration. The voltage is determined at each point, and the current density at the measurement site is calculated using known values for distance from the embryo and the resistivity of the bathing medium. As would be predicted from the spatial variation of TEP illustrated in *A* and *B*, there is outward current at the lateral edges of the neural ridges, inward current at the center of the neural groove, inward current at the lateral skin, and a large outward current at the blastopore.

around the outside of the embryonic skin. This technique uses a vibrating microelectrode (90, 91) that is driven at 300 Hz between two extreme positions roughly 20 μm apart. With the vibrating microelectrode placed close to an embryo within an electrically conducting medium and all signals filtered out other than those at 300 Hz, the probe records the voltage at the two extremes of its excursion, close to and more distant from the skin surface (Fig. 4*D*). With the use of the resistivity of the medium bathing the embryo, the differential voltage signals between the extremes of vibration are converted to current flowing in or out of the embryo at one point. Moving the location of the probe allows current flow to be mapped spatially around an embryo. Currents of 100 μA/cm^2 have been measured exiting the blastopore in *Xenopus* embryos at developmental stages 15–20 (a period spanning the formation of the neural tube; Fig. 4*D*) (84). The size of these measured currents is consistent with the rostrocaudal and mediolateral TEP gradients described in Figure 4. Since the resistivity of soft tissues is ~1,000 $\Omega \cdot$ cm, current densities of 100 μA/cm^2 give rise to voltage gradients of ~10 mV/mm. Importantly, the anterior neural folds also are sites of current exit, and here current densities of 2 μA/cm^2 have been measured. The sites of current leaks are regions of major tissue movements (173). Because tissue movements disrupt tight junctional seals transiently (47) and therefore reduce tissue resistivity locally (but not in distal areas), current flows parallel to the tightly sealed epithelium in areas of high resistivity (intact tight junctions) and exits the embryo in regions of low resistivity (where tight junctions have broken down) (Fig. 4*D*).

Although these two techniques demonstrate clearly that electrical signals exist during neurulation in amphibians, the signals at the blastopore and at the neural folds may have different functions. This is because the blas-

topore current persists after closure of the neural tube, but the rostrocaudal and mediolateral voltage gradients at the buckling neural plate stage disappear as the neural folds fuse at the end of neurulation (Fig. 5). The functional significance of switching spatially localized DC EFs on and off during gastrulation and neurulation, which are major developmental milestones, has been tested.

2. *Disrupting the natural EFs in amphibians disrupts development*

If the EFs in embryos play a significant role in development, disrupting the normal electrical milieu of embryos would cause developmental defects. This has been tested directly in amphibians using two experimental approaches. The first involved placing whole axolotl embryos in an externally applied EF of physiological magnitude for a period spanning either gastrulation or neurulation (~18–22 h). The applied EF was designed to disrupt the pattern and magnitude of the endogenous EFs by altering the TEP in a predictable way (139).

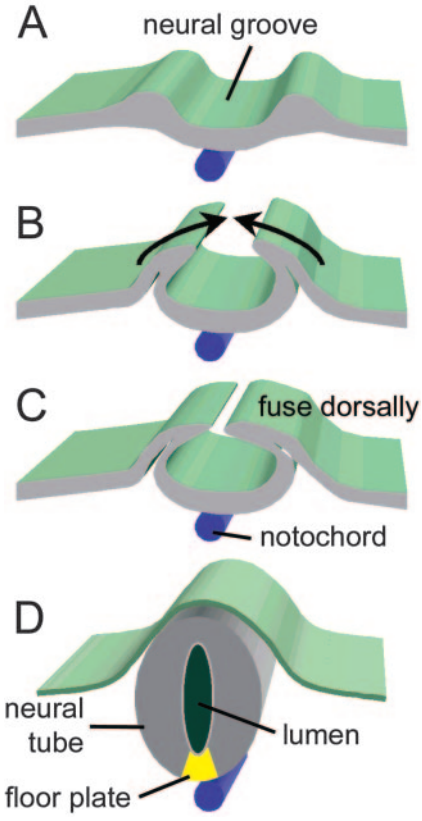

FIG. 5. Neural tube development. *A*: neural tube formation begins with a thickening of the ectoderm at the dorsal midline to form a neural groove flanked by raised neural ridges. *B*: the neural ridges fold upward gradually. *C*: eventually they fuse at the dorsal midline. *D*: after fusion the neural tube is a distinct structure, covered by a continuous epithelium (green). The resulting neural tube is therefore derived from the ectoderm in such a way that the lumen of the neural tube is historically the equivalent of the apical side of the ion-transporting embryonic epidermis. Note that the walls of the neural tube are thicker laterally and thinner ventrally at the floor plate (yellow), nearest to the notochord.

With no EF exposure (normal TEP), abnormalities occurred in no more than 17% of embryos. In embryos with no specific orientation to the imposed EF, 62% developed abnormally in an EF of 75 mV/mm and 43% at 50 mV/mm. Because the main axes of the measured endogenous voltage gradients run rostrocaudally and mediolaterally within the neural plate (Fig. 4), experiments were made using embryos with these body axes aligned with the EF vector. When the EF was imposed during neurulation with a cathode at the rostral end of the embryos, 95% (19/20) developed abnormally. When the cathode was caudal, 93% were abnormal, and of those with the long (rostrocaudal) embryonic axis perpendicular to the applied EF, 75% (12/16) were abnormal. The types of defects seen were profound and included absence of the cranium, loss of one or both eyes, a misshapen head, abnormal or absent brachial development, and incomplete closure of the neural folds in focused areas. In some cases, cells from the neural plate migrated out from the embryo onto the dish and continued to develop autonomously. In another experiment an EF of identical duration and magnitude was applied to embryos undergoing gastrulation. The EF was switched off at the end of gastrulation, and the embryos were allowed to develop to stage 36. Importantly, these embryos developed completely normally.

Interestingly, the polarity of the applied EF predicted the polarity of the developmental abnormalities that were induced. The most striking disruptions were seen in areas facing a cathode, where the skin TEP had become hyperpolarized. When the rostral (head) end of the embryo faced the cathode, head defects predominated, and when the caudal (tail) end of the embryo faced the cathode, lower abdominal and tail defects predominated (139).

The disruption to the embryonic skin TEP by applying an EF externally was marked and was polarized in a predictable manner. The TEP, which is normally internally positive, depolarized and switched polarity to become increasingly negative internally in regions of skin at the anode in an EF of 25–100 mV/mm. At the other end of the embryo, the TEP of skin under the cathode hyperpolarized and became increasingly more positive internally. Because the TEP was altered in this striking manner by the externally applied EF, the endogenous gradients of extracellular voltage under the skin will be scrambled by this imposed applied EF.

These experiments allow three conclusions. *1*) Endogenous EFs with normal polarity and magnitude are essential for normal development of the nervous system and other tissues. *2*) There was no generalized harmful effect of an applied EF since embryos exposed at gastrulation developed normally. *3*) Embryos responded to scrambling of their endogenous EF only during the period when cells were undergoing neurulation. This suggests

that neuronal cells gain and then lose the ability to respond to an applied EF during a specific window of developmental time.

The second approach to modifying endogenous EFs involved impaling *Xenopus* embryos with glass microelectrodes, similar to those used to measure the TEP. Current was passed through the electrodes so that the endogenous current leaving the blastopore was reduced or reversed (84). The effect of injecting current on the magnitude of the blastopore currents was measured directly using the vibrating microprobe. Injected current at 100 nA nulled the blastopore current, and 500 nA approximately reversed it. Eighty-seven percent of embryos (20/23) injected with this level of current for 9–11 h at stage 14–16 showed gross external developmental abnormalities. These included the formation of ventral pigmented bulges, failure of the anterior neural tube to close, reduced head development, retarded eye formation, the extrusion of cells from the blastopore into the dish, and failure of embryos to form functional cilia. Control embryos with long-term impalement of an electrode in the same region but no current, those with low current (10 nA, which did not affect the magnitude of the natural blastopore current), or those with reversed current that augmented the blastopore current, showed a much lower rate of abnormality.

Therefore, although two markedly different methods have been used to disrupt the endogenous EFs of amphibian embryos, they nevertheless induced a surprisingly uniform and striking array of developmental defects. Brain and tail structures were especially vulnerable and, significantly, these are regions of endogenous outward currents and of measurable steady DC voltage gradients in the embryo. The high incidence of neural tube defects also may be significant. Mutations in a number of genes such as sonic hedgehog cause neural tube defects (41), so it would be instructive to determine the expression levels of these genes in normal embryos and in embryos where the endogenous EFs have been disrupted. Conversely, it would be useful to determine whether disruption of endogenous EF affects expression patterns of key developmental genes.

One interpretation of the experiments outlined above is that steady voltage gradients within embryos provide a gross template for the development of pattern during ontogeny and that developmental abnormalities resulted from experimentally scrambling electrical cues necessary for patterning and cell migration within the embryo.

3. *Endogenous currents and voltage gradients are present in chick embryo: disrupting these disrupts development*

Importantly, currents and voltage gradients that are analogous to the blastopore and neural fold currents in amphibians have been measured in chick embryos (81). In stage 15–22 chick embryos, ionic currents greater than 100 μA/cm^2 leave the embryo via the posterior intestinal portal (PIP). This is the period of tail gut reduction; when there is extensive cell death at the caudal end of the embryo. The PIP is the opening into the hindgut from the yolk sac. These currents enter through the ectoderm of the embryo and upon flowing through the embryo generate a caudally negative voltage gradient of ~20 mV/mm. If these voltage gradients play a necessary role in embryogenesis, then disrupting them should alter development. This has been tested by creating an alternative path for current flow out of the embryo. Hollow capillaries that formed an ectopic region of low resistance were implanted to create, in effect, a permanent, nonhealing wound (83). This procedure reduced the magnitude and altered the internal pattern of the natural EF. Conductive implants designed to shunt currents out of the embryo were placed under the dorsal skin at the midtrunk level (stage 11–15). These hollow capillary shunts were ~100 μm outside diameter and 1 mm long and were filled with saline, in some cases gelled with 2% agarose to control against bulk fluid transfer between the embryo and its surroundings. They were placed perpendicular to the neural tube in a slit ~250 μm long and inserted around 500 μm under the ectodermal epithelium parallel to the neural axis. Currents of 18 μA/cm^2 left the conductive shunts. The net effect was to reduce the current leaving the PIP of these embryos by 30%. Ninety-two percent (25/27) of these embryos developed with gross abnormalities. The most common defect was in tail development, with the neural tube, notochord, and somites all either missing or truncated in the tail region. There were defects also in limb and head/brain development, but the frequency of defects increased in a rostrocaudal direction. Forty-four percent of embryos showed multiple developmental defects. Nonconductive, solid rod implants of the same dimensions were used in control embryos. No currents were measured escaping from these implants, nor did the implants influence the magnitude of the currents leaving the PIP. Only 11% (2/18) of control embryos with solid implants showed any developmental abnormalities; all the others developed completely normally, despite the continuous presence of the nonconducting implant. The abnormalities seen in experimental embryos were very similar to those produced in *rumpless* chicks, a naturally occurring mutation which can result in complete absence of all caudal structures (228). Vibrating probe measurements from *rumpless* chicks showed that currents leaving the PIP were ~41% of the PIP current in normal embryos (83), suggesting that this electrical deficit contributes, at least in part, to the tail structure deletions.

Several aspects of these experiments are important. *1*) They confirm that currents and endogenous voltage gradients are present during major episodes of chick de-

velopment and are greatest in the tail region. *2*) Reducing the PIP currents by shunting current out at an ectopic dorsal location has the greatest developmentally disruptive effect in the tail region. *3*) The shunt placement is several millimeters away from the site of the main defects, indicating that current shunting did not have nonspecific and deleterious local effects. *4*) Solid shunts had no effect. *5*) A naturally occurring chick mutation may cause tail deformities because of aberrant electrical signals.

A further point of interest and one which requires further study is that the primitive streak of the chick embryo, which is analogous to the amphibian blastopore, also is a site of large outward currents of ~100 μA/cm^2 (94). A physiological role for these currents has not been explored.

4. A voltage gradient exists across the neural tube and neuroblasts differentiate in this gradient

The vertebrate neural tube forms when the lateral edges of the neural plate thicken, rise up, and fold over to fuse with each other at the dorsal midline (Fig. 5). A hollow tube called the neural tube that develops to become the brain and spinal cord forms from the folded ectoderm and then detaches to lie below the skin. The luminal surface of the neural tube therefore is equivalent to the outer surface of embryonic skin. Because spatial and temporal differences in the electrical properties of embryonic skin generate steady endogenous electrical signals (see above), the neural tube has been investigated to determine whether similar electrical signals are generated across its wall. Amphibian neural tube does establish a potential difference across its wall known as the trans-neural tube potential (TNTP; Fig. 6) (82, 179). In axolotl this may be as large as 90 mV, with the lumen negative with respect to the extracellular space at stage 28. Because the wall of the neural tube is roughly 50 μm wide, this large potential difference would create a steady voltage gradient across cells in the neural tube wall of a remarkable 1,800 mV/mm [90 mV/50 μm = 180 mV/100 μm = 1,800 mV/mm]. The neuroblasts (neuronal precursors) within the wall must migrate, differentiate, and sprout directed axonal projections whilst exposed to this high, continuous extracellular EF. The TNTP is largely the result of transporting Na^+ out of the lumen, and this can be prevented pharmacologically by injecting benzamil or amiloride into the lumen. When this was done in axolotl embryos at stage 21–23 and the embryos were allowed to

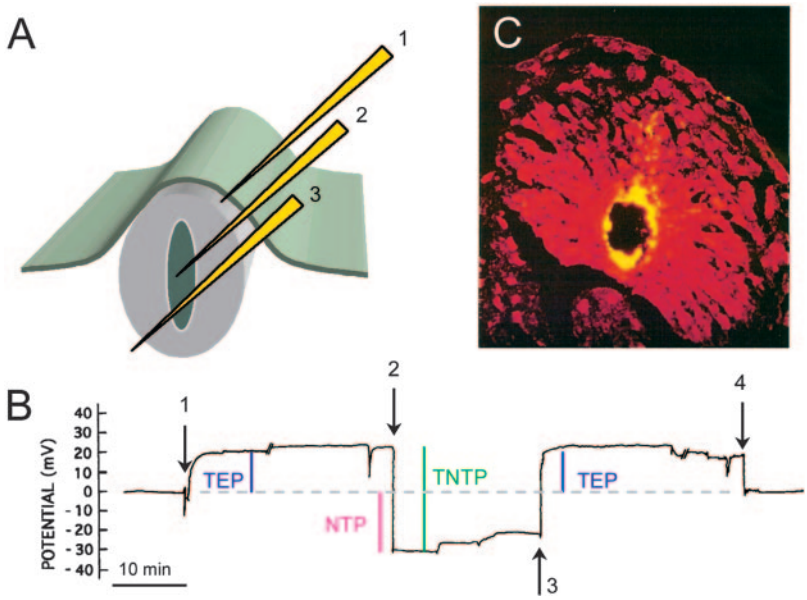

FIG. 6. Measurement of the *trans*-neural tube potential (TNTP) in an axolotl embryo by steady advance of a glass voltage-sensing electrode. *A*: initially the electrode penetrates the ectoderm (*1*) and records the TEP. It then advances through the wall of the neural tube, resting in the lumen (*2*) to record the neural tube potential (NTP). Then the electrode penetrates the far side of the neural tube to again record the TEP (*3*). The diagram shows the recording position of the tip of a single electrode as it advances through the tissue layers. *B*: a sample recording from the experiment described in *A*. Penetration of the ectoderm (*1*) indicates a TEP (blue bar) of ~20 mV, inside positive (relative to a reference electrode in the bath). At *2*, the electrode penetrates into the lumen of the neural tube, recording the NTP. The sharp downward deflection indicates that the lumen is negative (−30 mV) relative to the bath (pink bar). The sum of the TEP and NTP represents the TNTP (green bar). In this example the TNTP is about −50 mV (lumen negative relative to the outside of the neural tube). When the electrode tip is advanced out of the lumen through the far wall of the neural tube (*3*), there is a sharp upward deflection, in which the TEP of −20 mV is recorded again (second blue bar). At *4*, the electrode is withdrawn from the embryo. There is a sharp return to the reference baseline, which has remained stable throughout the experiment. *C*: a cross-section through a stage 23 axolotl embryo. To confirm that the electrode was positioned in the neural tube lumen, a fluorescent label (TRITC-con A) was iontophoresed into the neural tube from the same electrode used to measure the NTP at *point 2* above. [*B* and *C* redrawn from Shi and Borgens (179).]

develop for 36–52 h, by which time uninjected embryos had developed to stage 34–36, the TNTP collapsed for several hours. In all of 28 embryos tested, collapse of the TNTP caused major abnormalities in cranial and central nervous system (CNS) development. The defects were characterized by a disaggregation of cells from structures that had already begun to form (26). The cells that had comprised the optic and otic primordia, brain, neural tube, and notochord disaggregated, but did not die, whilst new internal structures failed to form. In effect, the internal structure of most embryos had been reduced to a formless mass of apparently dedifferentiated cells, simply by collapsing the TNTP. Remarkably, the external form of some embryos with collapsed TNTP continued to develop, despite the complete absence of concomitant internal histogenesis (26). Making similar injections of a vehicle solution into the neural tube, or of the active agents amiloride, or benzamil beneath the embryonic skin immediately adjacent to the neural tube had no effect on the TNTP and did not disturb development. This shows that neither the injection, nor the drugs, had a generalized toxic effect on the embryos and that the disaggregation of the neural tube and other internal structures was a consequence of collapse of the TNTP.

The presence of a strong electrical gradient across the wall of the neural tube and its role in maintaining the development of the neural tube itself (and other internal organ systems) are surprising findings with profound implications. These include *1*) the voltage drop across the wall of the neural tube will not be uniform, but will be steepest across the cells lining the lumen of the neural tube, because this region of tight junctional sealing is the area with the highest electrical resistance. Division and differentiation of presumptive CNS neurons begins at the lumen, and intriguingly, we have shown that the axis of cell division can be determined by applied and endogenous EFs an order of magnitude less than those across the neural tube (220, 184; see below). The axis of presumptive neuroblast cell division is regulated developmentally by segregating and polarizing a variety of proteins (e.g., numb, miranda, prospero) within neuroblasts as they prepare to divide. It would be worth testing whether the polar distribution of these molecules, which determines the axis of neuroblast division, is determined by the polarity of the TNTP. *2*) Because the neural tube varies in thickness, the largest EF (given a spatially uniform TNTP) will be across the thinnest region of the wall, which is the floor plate. This is an area of key importance in CNS patterning and neuronal differentiation. *3*) Finally, the number of neuroblasts that are stimulated to develop in culture increases markedly when a small DC EF is applied across these cells. Borgens suggests that this could be because culturing developing neurons without a weak polarized gradient of voltage imposed across them does not adequately mimic their in vivo environment (26).

In short, vertebrate embryos possess steady voltage gradients, particularly in areas where major developmental events related to cell movement and cell division are occurring. Disrupting these electrical fields disrupts normal development.

B. Example 2: Wounded Epithelia Generate a Steady EF That Controls Wound Healing

The second example of a tissue in which a steady DC EF is found extracellularly is wounded epithelium. Skin and cornea are well-studied examples (8, 36). However, all epithelia that segregate ions to establish a TEP will generate a wound-induced EF for the reasons outlined below.

The stratified mammalian cornea supports a transcorneal potential difference (TCPD) of around +30 to +40 mV, internally positive (Fig. 7*A*). The outer cells of the corneal epithelium are connected by tight junctions, as in amphibian skin, and these form the major electrical resistive barrier. Intact mammalian corneal epithelium transports Na^+ and K^+ inwards from tear fluid to extracellular fluid. Cl^- is transported in the opposite direction, out of the extracellular fluid into the tear fluid (34, 99). This separation of charge establishes the TCPD. Wounding the epithelial sheet creates a hole that breaches the high electrical resistance established by the tight junctions, and this short-circuits the epithelium, locally. The TCPD therefore drops to zero at the wound (Fig. 7*B*). However, because normal ion transport continues in unwounded epithelial cells behind the wound edge, the TCPD remains at normal values around 500–1,000 μm back from the wound. It is this gradient of electrical potential, 0 mV at the short-circuited lesion, +40 mV 500–1,000 μm back in unwounded tissue, that establishes a steady, laterally oriented EF with the cathode at the wound (Fig. 7*B*). So, in contrast to the TCPD generated across the intact epithelium, which has an apical to basal orientation, the wound-induced EF has a vector orthogonal to this. It runs laterally under the basal surfaces of the epithelial cells and returns laterally within the tear film across the apical surface of the epithelium (Fig. 7*B*). Mammalian skin also supports a TEP. When the skin is cut, a wound-induced EF arises immediately for the same reasons as in cornea (compare Fig. 7, *C* and *D*). Importantly, the wound-induced EF persists until the migrating epithelium reseals the wound and reestablishes a uniformly high electrical resistance, at which point the wound-induced EF drops to zero.

Two studies have confirmed experimentally the existence of steady wound-induced EFs. Cuts were made in bovine cornea and in guinea pig and human skin, and the potential difference across the epithelium at different distances back from the wound edge was measured directly using glass microelectrodes. In skin, the peak volt-

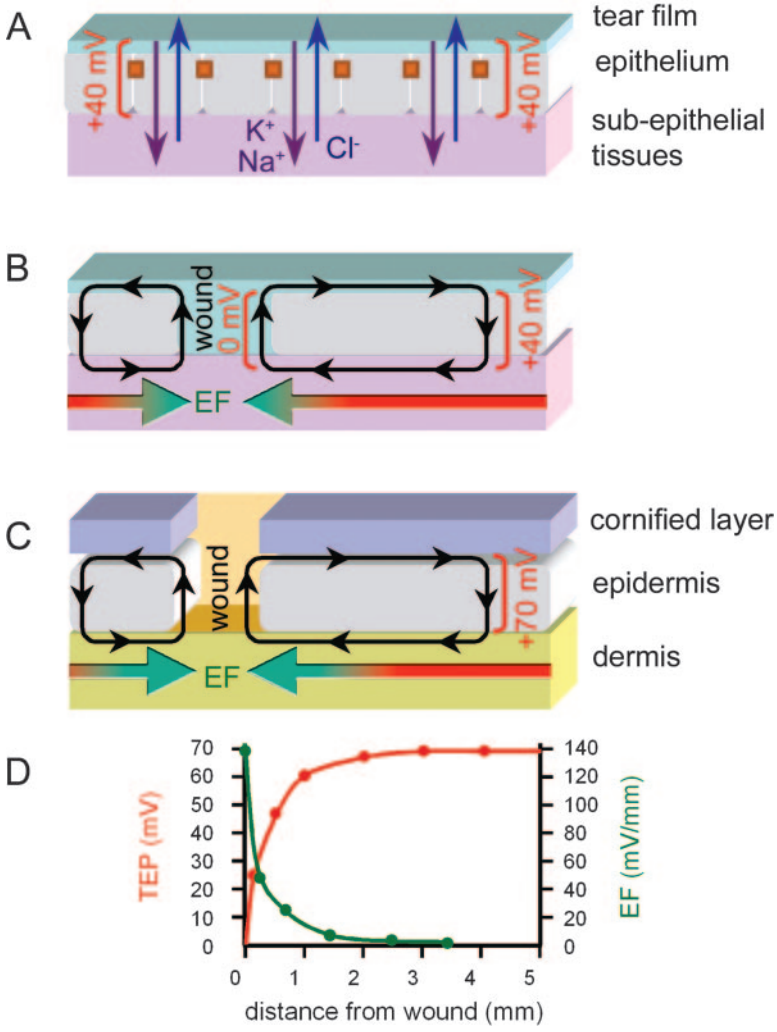

FIG. 7. Wounding collapses the TEP locally, resulting in an electric field lateral to the plane of the epithelium. *A*: intact mammalian corneal epithelium maintains a uniform TEP of +40 mV. This results from net inward transport of K^+ and Na^+ from the tear fluid (purple arrows) and the net outward transport of Cl^- from the cornea into the tear fluid (blue arrows). The TEP is maintained by the presence of tight junctions (orange squares). *B*: upon wounding, the epithelial seal is broken. The TEP collapses catastrophically to 0 mV at the wound, and ions immediately begin to leak out establishing an injury current (black arrows), which persists until the leak is sealed by reepithelialization. The TEP is maintained distally at +40 mV however, and this gradient of electrical potential establishes an EF within corneal tissues (horizontal arrow). *C*: ion transport (predominantly inward transport of Na^+) properties of mammalian skin also result in a substantial TEP, which establishes an injury current (black arrows) upon wounding and an electric field within the subepithelial tissues (horizontal arrow). In this case the return path for the current is in the layer between the dead, cornified tissue and the living epidermis. *D*: direct measurements of mammalian skin TEP (red line) as a function of distance from the wound edge. The EF (green line) resulting from the TEP gradient is 140 mV/mm very near the wound edge. The color gradients of the EF arrows in *C* and *D* indicate that the EF is strongest very near the wound and that the potential gradient (hence EF) is steeper in the mammalian skin wound than in the corneal wound, where the TEP is smaller. Therefore, the gradient of TEP per unit distance would be expected to be smaller in the cornea. [*D* redrawn from Vanable (197).]

age gradient at the wound edge was 140 mV/mm (Fig. 7*D*) (8) and in cornea 42 mV/mm, although the latter is an underestimate (36). In both tissues the voltage gradient dropped off exponentially from the wound edge with a profile that was formally equivalent to that of a uniform cable that has been disturbed at one point (Fig. 7*D*). The length constant for skin was ~0.3 mm, which means that at 330 μm back from the wound edge the voltage gradient would have decayed to 1/*e*, or 37%, of its maximum value at the wound edge. Direct measurements in skin showed voltage gradients of 140 mV/mm in the first 250 μm, 40 mV/mm between 300 and 500 μm, and around 10 mV/mm at 500–1,000 μm from the wound edge (8).

These findings have several important implications. *1*) All cell behaviors within ~500 μm of a wound edge in skin and cornea (and probably any ion-transporting epithelium; gut, for example) inevitably take place within a standing gradient of voltage. These include epithelial cell migration, epithelial cell division, nerve sprouting, leukocyte infiltration, and endothelial cell remodeling with associated angiogenesis; in short, the whole gamut of cellular responses to injury! *2*) Because of the exponential drop in voltage gradient with distance from a wound, any cell behaviors governed by the endogenous EF would be regulated differentially with distance from the wound. *3*) Increasing or decreasing the TEP would inevitably increase and decrease the voltage gradient profile at the wound.

In light of these issues, we have been studying the cell physiology at experimental wounds made in rat cornea in vivo. We have shown that a diverse array of inter-related cell behaviors is controlled by the endogenous EF at corneal wounds. These include directed migration into the wound of epithelial cells, the proliferation of epithelial cells, the axis of division of epithelial cells, the proportion of nerves sprouting at the wound, and the directional growth of nerve sprouts towards the wound edge (184, 185, 130).

1. *Wound healing is regulated by the wound-induced EF in rat cornea*

Increasing or decreasing the TCPD pharmacologically has the inevitable consequence of increasing or re-

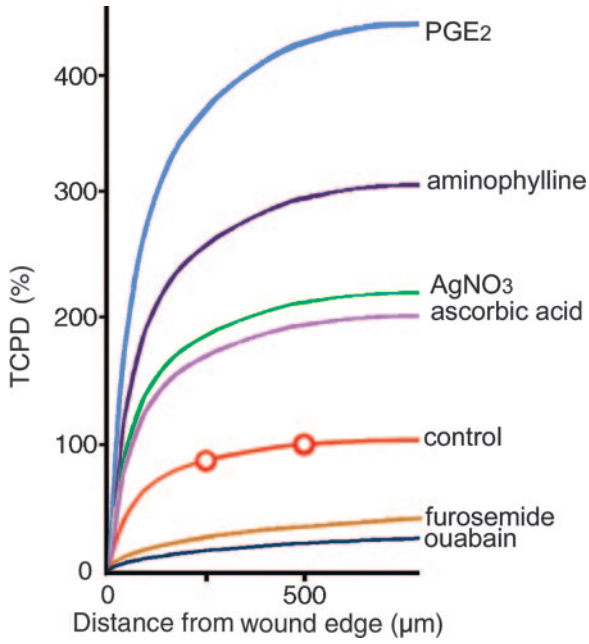

FIG. 8. The TCPD can be manipulated pharmacologically, and this provides a method for altering the wound-induced lateral EF predictably. Control plot (red) represents directly measured data, with 100% of the normal TCPD present 500 μm from the wound edge. The effects of various drugs are shown. For example, prostaglandin E_2 (PGE_2) increased the TCPD more than fourfold (425%). The drop off with distance to the wound is inferred by comparison with the no drug control graph. PGE_2 enhances chloride efflux, aminophylline and ascorbic acid inhibit phosphodiesterase breakdown of cAMP, which also enhances Cl^- efflux, and $AgNO_3$ increases both early Na^+ uptake and later Cl^- efflux (see Refs. 9, 31, 35, 100). These four drugs therefore have a common end point despite their different cellular actions and that is to increase the TCPD and therefore to proportionately increase the wound-induced EF (see Ref. 185). [Redrawn from Chiang et al. (36).]

ducing the wound-induced EF. We chose to modulate the TCPD using six different chemicals that act by different cellular mechanisms but whose only common effect was to change the TCPD (Fig. 8 and Ref. 185). In rat corneas treated with PGE_2 (0.1 mM), which increases Cl^- efflux, or with aminophylline (10 mM), which inhibits phosphodiesterase breakdown of cAMP and enhances Cl^- efflux, the TCPD increased three- to fourfold. Wounds treated with these drugs healed 2.5 times faster within the first 10 h than control wounds (184). In contrast, wounds treated with the Na^+-K^+-ATPase inhibitor ouabain (10 mM), which reduced the TCPD fivefold to 18% of normal, showed markedly slower wound healing (Fig. 9). The rate of wound healing was directly proportional to the size of the TCPD and therefore to the size of the wound-induced EF (185).

The natural EF present at experimental wounds in the isolated bovine eye also regulates wound healing (191). Reducing the natural EF with the Na^+ channel blocker benzamil (30 mM), or with Na^+-free physiological saline, slowed wound healing. The addition of injected current to restore and amplify the endogenous EF at wounds in Na^+-free medium, enhanced wound healing (191).

2. *Proliferation of epithelial cells is regulated by a physiological EF in vivo*

One element of the modulated wound healing response in cornea is due to EF-regulated proliferation of epithelial cells. We tested also whether epithelial cell proliferation is regulated electrically. Cell division is rare in the central area of unwounded corneal epithelium. In contrast, most cell division takes place within a peripheral ring of stem cells called the limbus. To provide cells for epithelial turnover, limbal stem cells differentiate and migrate within the basal layer of corneal epithelium and then move up through the epithelium to the surface layer (43). Wounding the corneal epithelium stimulates epithelial cells near the lesion to divide. Enhancing the endogenous wound-induced EF with PGE_2 or aminophylline induced a 40% increase in cell divisions within 600 μm of the wound edge, and suppressing the EF with ouabain caused a 27% suppression of mitoses (Fig. 10) (184). Manipulating the EF therefore clearly regulated the cell cycle and altered the frequency of cell division. Because this will also modulate the population pressure of cells within the epithelium, this could contribute to the rate of wound healing.

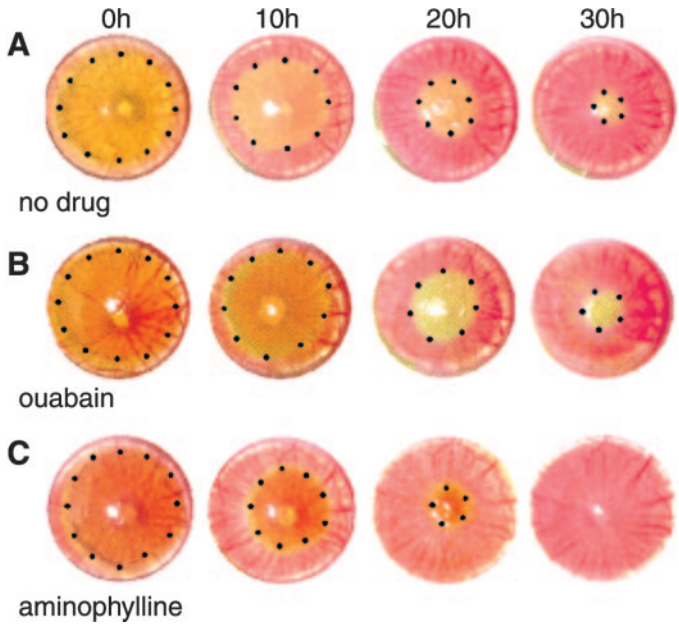

FIG. 9. Closure of wounds in rat cornea is controlled by naturally occurring wound-induced electrical signals. *A*: 4-mm circular lesions outlined by black dots and stained yellow with fluorescein take in excess of 30 h to close in untreated corneas. *B*: in corneas where the electrical signal is inhibited with ouabain (or furosemide, data not shown), wound healing is delayed. *C*: in corneas treated with aminophylline (and 3 other drugs not shown), which enhances the wound-induced electrical signal, healing is much faster, and by 20 h wounds are almost closed. [Modified from Song et al. (184).]

3. The axis of cell division is regulated by a physiological EF in vivo

Cultured corneal epithelial cells divide along a cleavage plane that forms perpendicular to the EF vector (220), in other words the mitotic spindle aligns parallel to the EF before cytokinesis. The reasons for this are completely unknown. Importantly, however, the same striking phenomenon occurs in vivo (184). In untreated corneal wounds, which generate their own endogenous EF, the mitotic spindles lie roughly parallel to the EF vector, with cleavage occurring perpendicular to this (Fig. 10*A*). Enhancing the wound-generated EF with PGE_2 or aminophylline roughly doubled the proportion of dividing cells whose cleavage planes were perpendicular to the EF vector. In contrast, reducing the wound-generated EF to <20% of its endogenous value with ouabain (Fig. 10, *B* and *C*) abolished wound-oriented cell divisions.

If the endogenous EF in rat cornea is causal in directing the axis of cell division, then its effects should be highest at the wound edge and decline back from here, because the EF declines exponentially away from the wound. This is the case. Orientation of the mitotic spindle was strongest in the first 200 μm and roughly halved 200–400 μm back from the wound. By 600 μm back from the edge, the angle of the mitotic spindle was not different from those seen in the limbus (1,700 μm away); both were randomly oriented with respect to the wound-generated EF vector (184). Importantly, 600 μm corresponds to the measured distance that the EF penetrates into the tissue (see Fig. 7*D*). Oriented division therefore dropped to zero as a function of distance back from the wound edge, and there was no oriented division in the distant limbus where the EF would be zero.

Enhancing the EF with PGE_2 or aminophylline increased the orientation of cell division with significant orientation now occurring further from the wound edge, at 600 μm. Collapsing the EF with ouabain abolished oriented cell division, even within 200 μm of the wound edge. Clearly, the naturally occurring EF controls the orientation of cell divisions in vivo.

One clue to potential mechanisms indicates that phospholipid second messenger signals may transduce the EF into oriented cell division. This is because the aminoglycoside antibiotic neomycin, which had no effects on the TCPD (EF), but which inhibits phospholipase C, abolished oriented cell divisions in vivo. Interestingly, neomycin also prevents EF-induced orientation of embryonic myoblasts and of neuronal growth cones (58, 127).

It may be significant that a local environmental guidance cue (an EF) directs the plane of cell division. In the developing CNS for example, crucial decisions regarding the fate of neuroblasts and, consequently, the fundamental architecture of the brain are made by fixing the axis of neuroblast division. Symmetrical cleavage of progenitor cells in the ventricular zone with an axis that retains both daughters in the proliferative pool leads to reentry into the cell cycle and an exponential expansion of the ventricular zone population. In contrast, asymmetrical cell division with a cleavage plane parallel to the ventricular boundary releases one daughter cell from the cell cycle, and this cell differentiates and migrates away. Control over these events is exerted by a host of asymmetrically distributed protein molecules such as numb, miranda, prospero, and bazooka (74) and is determined in part by where the rotating mitotic spindle comes to rest (77). Whether the distribution of the determinative protein markers or the dynamics of spindle rotation and arrest are regulated by an endogenous or an applied EF remains to be determined.

4. Nerve growth is regulated by a physiological EF in vivo

Nerves sprout in response to wounds in skin (64, 117) and in cornea (10, 175). In cornea, with its rich sensory innervation, this is a biphasic process. Early collateral sprouts appear within only a few hours, mostly from intact fibers near the wound. In rabbit cornea these early collateral sprouts show a striking orientation with many parallel nerve bundles growing directly towards the wound edge (175). The early sprouts are transient and over the following 7 days or so, they retract and are replaced by regenerating neurites (10). The cues guiding growth cones of early sprouts directly towards the wound edge have not been explored. Electrical guidance of nerve growth cones has been proposed since the time of Cajal, a century ago, and there is much evidence for this robust phenomenon in tissue culture (see below). Because a corneal wound generates its own EF, we have tested the hypothesis that the wound-generated EF is causal in directing nerve sprouts to grow directly towards the wound edge. These experiments have provided clear evidence of a physiological role for electrical guidance of nerve growth in vivo (185). A 4-mm-long nasal to temporal slit wound was made in rat cornea. Early nerve sprouts are evident by 16 h, but they are not yet oriented with respect to the wound edge. Between 16 and 24 h, many more nerve sprouts appear, and most are perpendicular to the wound edge (Fig. 11). When the wound-generated EF was enhanced with PGE_2, aminophylline, $AgNO_3$, or ascorbic acid (Fig. 8), neurite growth towards the wound was enhanced. More sprouts appeared, sprouts appeared earlier, and sprouts oriented towards the wound edge earlier (within 16 h; Fig. 11). Collapsing the EF with ouabain or furosemide did not prevent early collateral nerve sprouting, but nerve growth was not directed towards the wound edge (Fig. 11) (185). This demonstration that both the magnitude of the sprouting response and the direc-

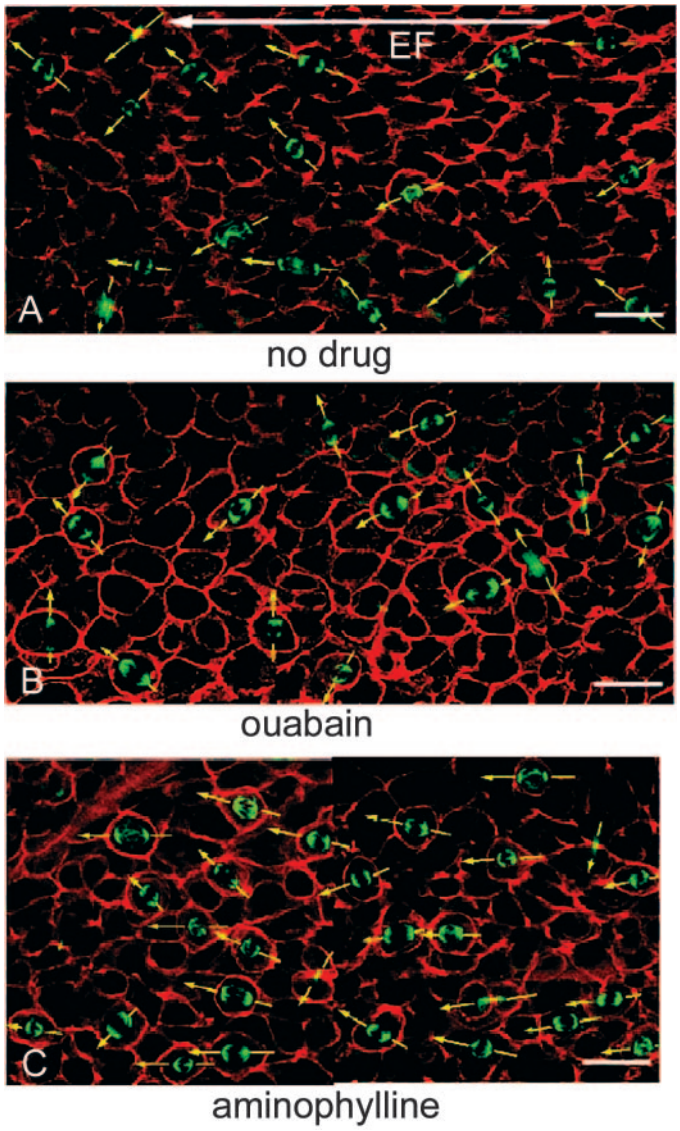

FIG. 10. Epithelial cell proliferation and the axis of cell division are controlled by naturally occurring wound-induced electrical signals. Mitotic profiles of corneal epithelial cells (green) in a whole mount rat cornea close to a wound edge (left margin). Wounding the cornea stimulates cell division near the wound edge, and the proportion of dividing cells drops off with distance back from the wound edge, as predicted if this were controlled by the wound-induced electrical signals. Enhancing these electrical signals pharmacologically, for example, with aminophylline, increased cell divisions (compare *A* with *C*), and suppressing the electrical signals with ouabain suppressed cell divisions (compare *A* and *C* with *B*). *A*: in untreated corneas, the long axis of the mitotic spindle (yellow arrows) was not oriented randomly, but lay significantly more parallel than perpendicular to the EF vector. *B*: in corneas where the electrical signal was suppressed with ouabain, the spindle axis was oriented randomly with respect to the EF vector. *C*: in corneas where the electrical signal was enhanced with aminophylline, the spindle axis was oriented strongly parallel to the EF vector. [Modified from Song et al. (184).]

tional growth of the nerve sprouts are controlled by the wound-generated EF is significant in several respects.

1) Effective wound healing in the cornea (and perhaps skin and other tissues) requires a normal sensory nerve supply and may depend on the biphasic reinnervation pattern described above. For example, corneal wound healing is compromised in patients with sensory neuropathy. The best known example is diabetes (67). These conditions are characterized by repeated attempts to reepithelialize the wound, but in the absence of concomitant reinnervation, healing is poor and the epithelium sloughs off repeatedly. This indicates that there are important neurotrophic interactions between the epithelial cells and the sensory nerves supplying the epithelium (11). Significantly, the early nerve sprouts that are directed towards the wound edge "appear to roll into the wound with the migrating epithelial cells" (175). Because electrical signals arise immediately at a wound and control multiple cell behaviors in vivo (cell proliferation, directed cell division, directed epithelial cell migration, and directed nerve sprouting), this suggests that the EF may orchestrate an integrated response of interdependent cell behaviors that includes the epithelial and nerve interactions essential for wound healing.

Wound healing clearly involves an array of regulatory and guidance cues, in addition to the electrical signal. It would be worth knowing whether the expression levels of

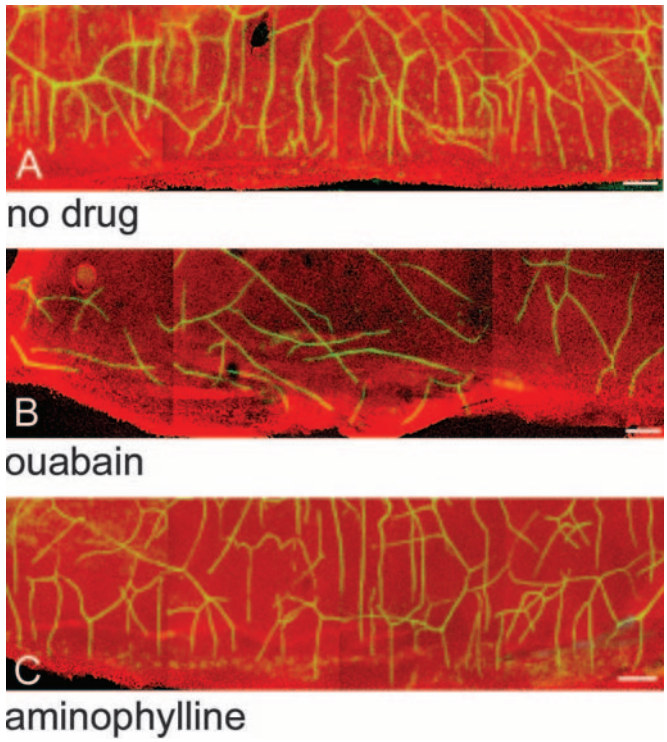

FIG. 11. Nerve sprouting is stimulated and directed by a wound-induced electrical signal in vivo. *A*: a wound in rat cornea attracts robust nerve sprouts within 24 h, and these are directed towards the wound edge. *B*: disrupting the wound-induced electrical field (with ouabain) did not prevent nerve sprouting, but sprouts were no longer directed by the EF vector towards the wound edge. *C*: enhancing the wound-induced electrical field (with aminophylline) increased and speeded up nerve sprouting along the EF vector towards the wound edge. [Modified from Song et al. (185).]

the multiple growth factors and cytokines that are released at epithelial wounds also are under electrical control (see also sect. v*C1*). In addition, we show below that at least in one respect (wound closure) the electrical signal can predominate over all others.

2) Because this work confirms the physiological relevance of an endogenous EF in directing nerve growth cones in vivo, a reevaluation of the importance of electrical cues in nerve guidance and how they interact with other coexisting guidance cues is warranted.

3) Because endogenous EFs play a physiological role in promoting and directing nerve growth cones, this strengthens the rationale for using an applied EF in therapies for neuronal regeneration (see sect. VI).

5. Electrically driven wound healing: closing remarks

Ion-transporting epithelia therefore generate a wound-induced electrical signal that lasts for many hours. This signal regulates different cell behaviors within 500 μm to 1 mm from the wound edge and does so until reepithelialization has occurred. Importantly, even transient breaches in an epithelium, for example, those created by local damage in the intestinal lining, or by apoptosis and natural turnover, will induce shorter-lived, local electrical signals, and these too may influence cell behaviors.

In addition, there are clear parallels between the critical problems faced by a wounded epithelial syncytium and those faced by a single cell with a hole in its membrane. In each case, the potential difference becomes short-circuited, either across the whole epithelial sheet, or across the single cell membrane (see Fig. 1, *E* and *F*). Both single cells and sheets of cells may use electrical strategies in mounting a wound-healing response. Crayfish giant axons rapidly seal holes in the plasmalemma, although the process is not immediate. In fact, the movement of dye particles into the cut axon gradually becomes restricted to molecules of progressively smaller size over about an hour. During this period, injury-induced vesicles accumulate at the cut end, interact, and form junctional complexes with each other and with the cut ends of the axolemma to create a functional plug. An ionic seal is formed in ~1 h as shown by the drop off in injury current at the cut end of the axon measured with a vibrating probe (53, 63). Vesicle accumulation is a Ca^{2+}-dependent process and is essential to prevent neuronal death and to allow axonal repair. Whether vesicle accumulation is triggered by the immediate collapse of the membrane potential and driven by the wound-induced voltage gradient in the terminal end of the axon has not been tested (22).

In evolutionary terms, membrane resealing to close an electrical leak is among the most primitive activities that cells undertake. Perhaps both single cells and sheets of cells use the instantaneous electrical signal induced by injury to seal a membrane and to close a wound, respectively.

Examples *1* and *2* above have introduced the existence of small EFs within the extracellular spaces and the evidence supporting physiological roles for these EFs in controlling cell behaviors in development and in wound healing. The likely mechanisms are discussed below. Mostly these do not involve the creation of voltage gradients across the cell cytoplasm, because the high resistance of the cell membrane prevents this from occurring. However, EFs do exist across the cytoplasm of cells joined by gap junctions or by cytoplasmic bridges. Two striking examples follow.

C. Example 3: The Establishment of Left-Right Organ Asymmetry

Intracellular/transcellular electrical signals may regulate the spatial expression of the genes that control embryonic development of left-right (L/R) organ asymmetry (109). A cascade of asymmetrically expressed or repressed genes precedes and directs the development of morphological asymmetries, although the early events that act upstream of asymmetric gene expression are less clear. For example in the chick, sonic hedgehog (Shh) initially is expressed symmetrically around Hensen's node. At stage 4 the expression becomes restricted to the left lateral plate mesoderm, and this is responsible for the later left-sided expression of nodal (108). The spatial asymmetries of gene expression take place within large groups of cells, and this suggests the involvement of long-range communications in setting up these asymmetries. Interestingly, these cells communicate with each other using gap junctions, and in *Xenopus* and chick this is essential for the development of proper L/R asymmetry. Blocking gap junctional communication with drugs, antibodies, or antisense oligonucleotides causes symmetrical expression of Shh and nodal and consequently a failure of L/R organ asymmetry (107, 106). Therefore, L/R asymmetry may require the biased movement of some morphogen through gap junctions to create an asymmetry of the signals that drive differential gene expression. A means of biasing morphogen diffusion through gap junctions to establish the signaling gradient also would be needed. Fluorescent dyes that report cell membrane potential show that a sharp asymmetry exists in epithelial membrane potential across the midline of the stage 2–4 chick embryo (109). Voltage gradients as large as 20 mV were measured, with cells on the left side of the midline depolarized with respect to those on the right side (Fig. 12). Pharmacological or genetic perturbation studies showed that the membrane potential asymmetry depended on the transporter function of the H^+-K^+-ATPase. Inhibition of

the H^+-K^+-ATPase randomized the expression of genes on either side of the midline and the distribution of internal organs (109). This work indicates clearly that there is an electrical component to the communication across the dorsal-ventral midline that establishes normal L/R organ asymmetry in chick and frog embryos. The sharp difference in membrane potential between the future left and right side of the embryo indicates that there is a voltage gradient within the cytoplasm of cells that communicate via gap junctions across the midline. Small charged molecules therefore could become distributed asymmetrically across the midline to direct the downstream events of asymmetric gene expression (Fig. 12). Two key questions arise: *1*) What are the early signals that induce the asymmetries in ion transport to create and maintain the voltage gradient? *2*) What molecule(s) that pass through gap junctions are distributed in response to the EF? This may link an EF-established chemical gradient to the later gene expression pattern. Candidate molecules have been proposed and include the usual second messenger suspects: Ca^{2+} , inositol phospholipids, and cyclic nucleotides.

D. Example 4: Intracellular Gradients of Potential Segregate Charged Proteins Within the Cytoplasm

Lionel Jaffe has pioneered the notion that transcellular ionic currents and voltage gradients may be an essential physiological step in establishing cytoplasmic polarity. Using eggs of the seaweed *Fucus*, he demonstrated the existence of transcellular currents that determine the prospective axis of germination (88). These currents are caused by a stabilized separation and accumulation of cation pumps on one side of the fertilized egg and of permeability channels on the opposite side. The accompanying EF gradient was proposed to have an electrophoretic effect on the distribution of charged morphogenetic determinants within the cytoplasm. This was seminal work, both practically, in demonstrating the existence of currents that determine embryonic polarity, and conceptually, in introducing the idea that gradients of electrical potential could direct the localization of cytoplasmic constituents.

The fourth example of a steady DC EF in a biological system provides strong evidence to support Jaffe's concept and comes from work on the insect oocyte-nurse cell complex. In the moth *Cecropia* this incompletely divided cell complex consists of an oocyte and seven nurse cells linked to each other by seven cytoplasmic bridges clustered in a complex at the center of the group (Fig. 13*A*). Remarkably, the cytoplasm of the oocyte is ~10 mV positive with respect to the cytoplasm of the nurse cells (210). Because the bridges are 30 μm wide and 50 μm long, this gradient of electrical potential creates a steady EF of ~200 mV/mm across the cytoplasmic bridges connecting oocyte and nurse cells. When fluorescently labeled proteins carrying positive or negative charges were injected into either the oocyte or the nurse cell, their diffusion within and through the bridges was determined by the polarity of the endogenous EF and the charge on the injected protein. Positively charged fluorescently labeled lysozyme (Fly) injected into the oocyte moved from oocyte to nurse cells, but did not cross the cytoplasmic bridge in the opposite direction, when injected into the nurse cells. The polarity of fluorescently labeled protein movement was completely reversed when the negatively charged methyl carboxylated lysozyme (MCFly) was used. MCFly could cross the bridges from nurse cell to oocyte, but not from oocyte to nurse cell. The endogenous EF therefore played a major role in determining the spatial distribution of injected charged proteins. An important question is whether soluble, endogenous protein molecules also are distributed electrophoretically. This has been studied in the 16-cell syncytium *Drosophila* follicle, which has a stable potential difference of 2.5 mV between nurse cells and oocytes (oocyte positive with respect to the nurse cell; Fig. 13*B*) and in which the injected proteins Fly and MCFly showed the same asymmetrically regu-

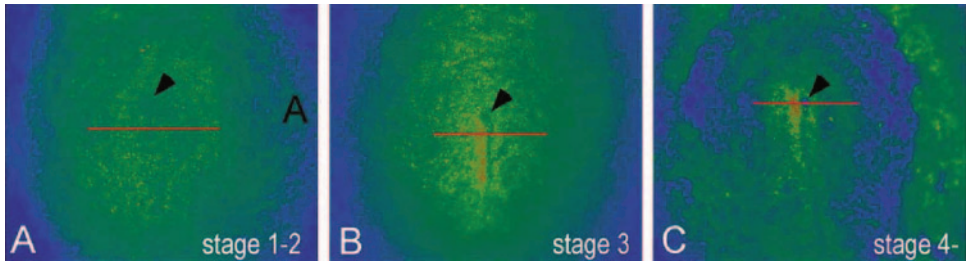

FIG. 12. Left/right (L/R) asymmetries of membrane potential patterns in the primitive streak area. A transient domain of depolarization to the left side of the primitive streak in chick embryos visualized with the potentiometric fluorescent probe $DiBAC_4$. The blue to green to red pseudo-color scale represents increasing fluorescence intensities reflecting increased accumulation of the anionic dye in intracellular membranes. Increased fluorescence corresponds to a less negative membrane potential (i.e., depolarized). [From Levin et al. (109).]

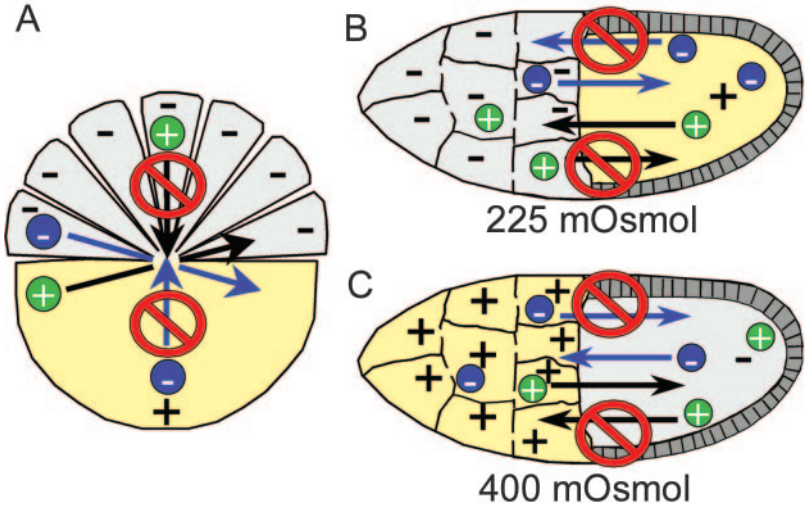

FIG. 13. Redistribution of charged molecules within the insect nurse cell (grey)/oocyte (yellow) syncytium. *A*: ovarian follicle of the moth *Cecropia*. Seven nurse cells are connected to the oocyte via a cytoplasmic bridge. *B*: ovarian follicle of the fruit fly *Drosophila*. Only 9 of the 15 nurse cells are shown. In *A* and *B*, the electrical potential of the oocyte is positive with respect to the follicle cells. Positively charged molecules injected into the oocyte move into the nurse cells as a result of the electric field across the cytoplasmic bridge, but when injected into the nurse cells, the same molecules did not move into the oocyte. Conversely, negatively charged molecules injected into the nurse cells move into the oocyte, but when injected into the oocyte they did not move into the nurse cells. The asymmetric distribution is a function of the potential difference in the two compartments. *C*: increasing the osmolarity of the extracellular medium from 250 mosM (physiological) to 400 mosM reverses the electrical potential of the *Drosophila* follicle. Two-dimensional gel electrophoresis of soluble proteins isolated from the cytoplasm nurse cells and oocytes indicates that charged endogenous proteins respond to the change in electrical potential in a manner consistent with their redistribution by the endogenous electrical gradient; that is, the direction of movement is opposite to that in *B*. (Based on Refs. 39, 209, 210.)

lated diffusion based on their respective charge (209). Unexpectedly and for unknown reasons, raising the medium osmolarity reversed the polarity of this gradient. Injected negatively charged Fly now accumulated in the nurse cells as opposed to the oocyte (183), thus providing a useful experimental tool. Using two-dimensional gel electrophoresis, 12 soluble acidic proteins and 7 soluble basic proteins were identified in both oocytes and nurse cells of *Drosophila* follicles. When the EF polarity across the nurse cell-oocyte cytoplasmic bridges was reversed, by increasing the medium osmolarity, such that the oocyte now was negative with respect to the nurse cells (Fig. 13*C*), the concentrations of all 12 acidic proteins in the nurse cells increased while 7 of the acidic proteins in the oocyte decreased. For the basic proteins, polarity reversal caused an increase in all seven proteins in the oocyte and four of the seven basic proteins decreased in the nurse cells. In short, the distribution of soluble endogenous proteins between oocyte and nurse cells could be modulated both by the charge on the protein and by the electrical polarity of the cytoplasmic bridges.

While these insect systems show substantial intercellular voltage gradients across their connecting cytoplasmic bridges, an even greater voltage drop has been reported between the oocyte and its single nurse cell in the marine worm *Ophryotrocha labronica*. Here a remarkable 22–32 mV difference exists across the 3-μm-wide cytoplasmic bridge (55).

V. HOW DO CELLS RESPOND TO PHYSIOLOGICAL ELECTRICAL FIELDS: PHENOMENOLOGY AND MECHANISMS

The ways in which a variety of different cell types respond to a physiological DC EF have been determined by mimicking the EF in tissue or organ culture. Such experiments are simple. They involve culturing cells in specially designed chambers connected to a DC power supply. However, there are important design features of the experimental set-up that are necessary to mimic the endogenous EF. Figure 14 shows the basic system. *1*) The culture chambers are of defined geometry. This allows the EF to be calculated easily and its vector to be controlled. *2*) The culture chambers are wafer thin, ~400 μm deep, as is the coverglass lid to the chamber. This ensures that heat dissipates from the medium as quickly as it builds up. Joule heating is proportional to the square of the current passing through a chamber. Maximizing the resistance across the chamber minimizes this current. Because this is proportional to chamber cross-sectional area, this is most easily minimized by minimizing the height of the chambers above the cells. Very thin chambers are best. We have confirmed this directly. Using a probe that could detect a 0.1°C change, there was no detectable change in temperature in chambers 0.4 mm deep exposed to a physiological EF of 185 mV/mm (126). *3*) Agar-gelled salt bridges connect the metal electrodes with the culture

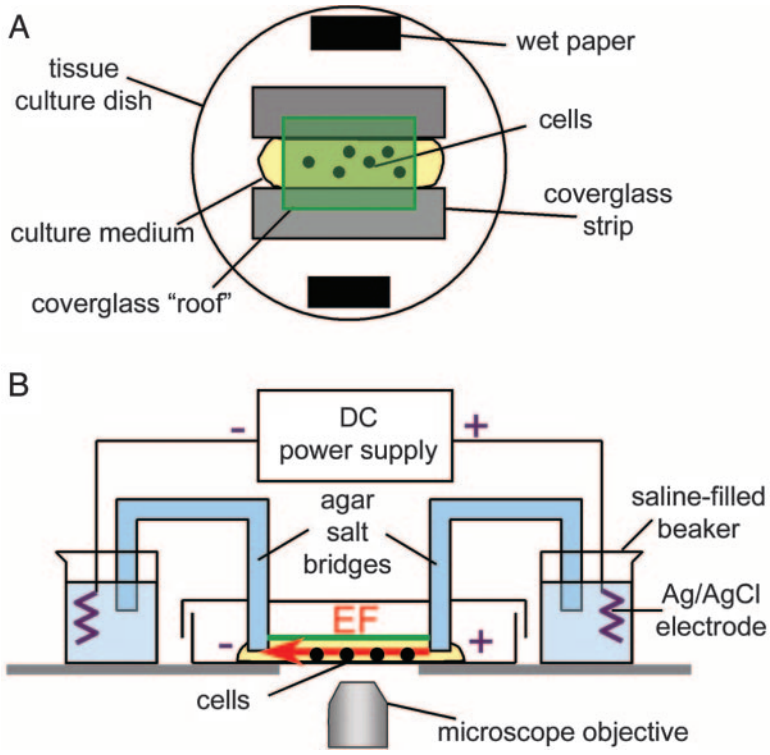

FIG. 14. Method of electric field application. *A*: top view of chamber. Chambers are made from standard 100-mm tissue-culture dishes. Two strips of number 1 coverglass are secured to the bottom of the dish parallel to each other, 1 cm apart. Cells are plated into the resulting trough, and another coverglass is secured over the top with silicone grease, spanning the entire trough. Strips of paper saturated with water are placed in the dish to maintain humidity. *B*: side view. Electrical contact is made to the chamber by inserting glass tubes filled with a salt solution gelled with 1% agar through holes in the lid of the chamber. One end of each tube rests in a pool of culture medium continuous with the medium in which the cells are growing; the other end of each tube is placed in a beaker of saline. Ag/AgCl electrodes in each beaker are attached to a direct-current (DC) power supply. Fine adjustments to the EF strength are made via a variable resistor in series with the power supply. Field strength is checked periodically by measuring the voltage drop across the length of the central trough directly using a voltmeter.

medium. This isolates cultures from potentially toxic electrode products. Many studies have used these well-established techniques (149, 171), and we review only a selection of them.

A. Nerve Growth Is Enhanced and Directed by an Applied EF

The notion that nerve growth could be directed using electrical signals is an old one, and the historical background is outlined fully elsewhere (120, 129). Briefly, the earliest attempt to test this experimentally was made by Ingvar in 1920 (86), shortly after the discovery of the tissue culture technique. Although no data or supporting pictures were presented, he reported that the growth of fibers from explanted chick brain tissue was along the lines of force of the galvanic field and that the processes growing anodally were morphologically different from those growing cathodally. Marsh and Beams (115) were the first to show convincing galvanotropic responses in 1946. At a threshold EF of 50–60 mV/mm, neurites from chick medullary explants grew and turned towards the cathode (115). This issue was resurrected in more recent studies that were controlled carefully as outlined above. At EF strengths >70 mV/mm, neurites from chick dorsal root ganglion explants grew about three times faster towards the cathode than the anode, but they did not turn (93).

1. Embryonic frog spinal neurons as a model system

Dissociated neurons from the neural tube of *Xenopus laevis* embryos have been used widely in studies of chemotropic growth cone guidance, and much is known regarding the receptor, second messenger, and cytoskeletal elements that transduce signals presented as chemical gradients, for example, neurotransmitters, neurotrophins, and netrins (186, 187). These cultures are not a homogeneous neuronal population, although ~80% of the earliest outgrowths from dissociated neural tubes of stage 17–22 embryos are cholinergic motoneurons (194). This preparation has been used to show that individual growth cones show striking turning responses in an applied EF of physiological strength (78, 156). The phenomenon is extremely robust and frequently more impressive than chemotropic turning (see movie 1, which is located at http://physrev.physiology.org/cgi/content/full/00020.2004/DC1). A physiological EF as low as 10 mV/mm (0.5 mV across a growth cone with a span of 50 μm) causes growth cones to turn, generally toward the cathode (Fig. 15*B*). In addition to directing the growth cone, an EF sculpts neuronal architecture by increasing and directing branching cathodally, by selectively pruning anodal facing processes, and by modulating growth rates according to EF polarity (faster cathodally) (119, 121, 122, 125). It is likely that these are primary responses to the EF because galvanotropic behavior persisted in cultures where medium was cross-perfused perpendicular to the EF vector (with complete exchange

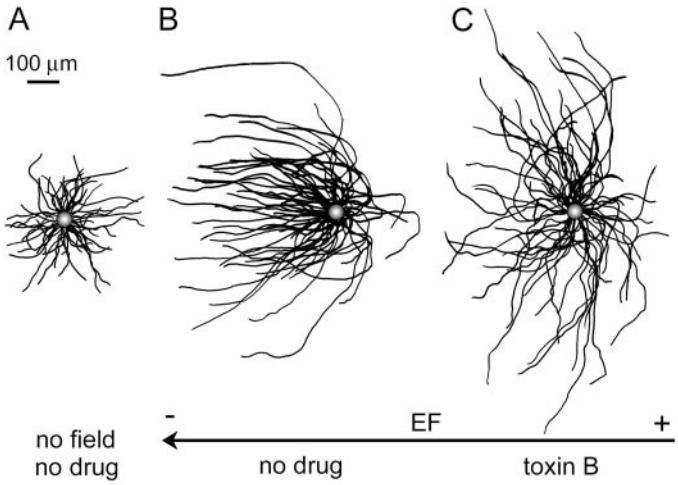

FIG. 15. *Xenopus* spinal neurons exposed to a physiological EF. Drawings were made by superimposing individual cell bodies (grey dots) of dissociated neurons and tracing the path taken by the growing neurite over 5 h of time-lapse observation. *A*: cells in the absence of an EF grow randomly in all directions. *B*: cells in an EF of 150 mV/mm grow dramatically toward the cathode, often turning through large angles. The rate of neurite growth is increased by the EF and is fastest toward the cathode. *C*: inhibition of the Rho family of small GTPases (rac, rho, and cdc42) with toxin B prevents cathodal orientation. The scale bar applies to all drawings.

every 10 min). This would minimize any possibility that the EF could induce a standing chemical or temperature gradient within the culture medium to which growth cones might respond (78).

Intriguingly, whether growth cones are attracted to or repelled by a cathode depends on the nerve cell type, the substratum, and whether the process is axonal or dendritic. Growth cones change their direction of migration in a DC EF depending on the substratum adhesivity and net charge (167). Sensory neurites do not turn (93), motor neurites turn cathodally (78), and PC12 neurites turn anodally (42). Moreover, embryonic rat hippocampal dendrites were attracted cathodally, but the axon on the same cell body did not turn (46). In one sense this is a bewildering situation. Alternatively, it indicates that neuronal responsiveness to the endogenous cues that nerves encounter both in development and during regeneration may involve complexities and subtleties still to be revealed.

2. Neuronal growth cone turning and induced receptor asymmetry

The most widely studied of the responses that growth cones show in an EF is cathodal turning. The mechanism underpinning this has been explored. Beginning at the receptor level, a physiological EF physically moves charged receptor molecules exposed on the outer surface of the lipid bilayer and creates receptor asymmetry between cathodal- and anodal-facing membranes (89, 163). An applied EF induces receptor asymmetries for the polysaccharide-binding plant lectins such as concanavalin A (conA) and for the neurotransmitter ACh on *Xenopus* myoblasts and on neurons (156, 162, 193). The epidermal growth factor (EGF) receptors on corneal epithelial cells (219) and on fibroblasts (73) also are redistributed by a physiological EF (Fig. 16). In each case fluorescently labeled receptors accumulated cathodally. In a high but still physiological EF of 500 mV/mm for 6 h, neuronal growth cones facing cathodally stained more intensely for fluorescently labeled conA receptors than growth cones facing anodally (156). Collectively, these findings are the basis for the untested assumption that even at a threshold EF strength as low as 10 mV/mm an EF induces receptor asymmetry across the span of a single neuronal growth cone (Fig. 17*A*). An induced asymmetry of receptors may be required for directed motility because binding of conA to neurons before EF application prevented both conA receptor redistribution and asymmetry and cathodal turning of the growth cone (123). The receptors may be unable to redistribute and accumulate cathodally because they have become immobilized by cross-linking with the tetrameric ligand (156). Receptors for several physiologically relevant neurotransmitters are present on embryonic *Xenopus* growth cones (158), which release neurotransmitters such as ACh spontaneously as they project towards their target tissues to form synapses (214). Because growth cones respond chemotropically to gradients of the neurotransmitters ACh (224) and glutamate (225), we tested the notion that in growth cones exposed to a

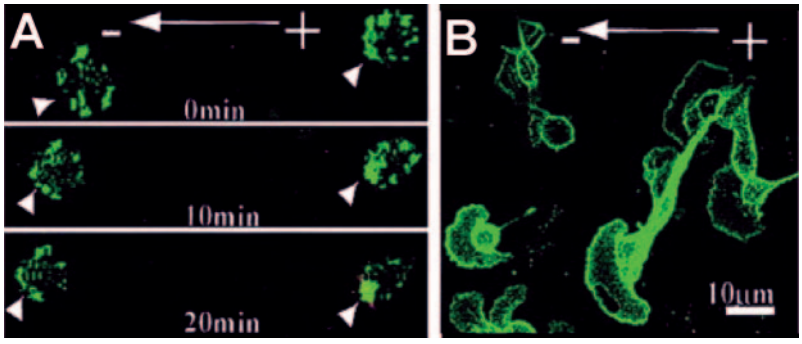

FIG. 16. Epidermal growth factor (EGF) receptors are redistributed to the cathodal side of migrating corneal epithelial cells. *A*: time lapse images show FITC-EGFR accumulated gradually to the cathodal side, within 10 min in an EF (300 mV/mm). *B*: FITC-EGFR accumulated cathodally at the leading edges of a number of cells (150 mV/mm, 1.5 h).

physiological EF, ACh release could activate asymmetrically distributed receptors to effect growth cone turning. In this scenario, the EF is transduced and its vector encoded by induced neurotransmitter receptor asymmetry (Fig. 17, *A* and *B*). Blocking activation of the neuronal nicotinic ACh receptor with D-tubocurare prevented cathodal turning, whilst the muscarinic ACh receptor antagonist atropine and suramin, which is an antagonist of both P2-purinoceptor and the basic fibroblast growth factor (bFGF) receptor, markedly enhanced cathodal turning at a given EF strength (57).

These observations indicate that *1*) neurotransmitters and EFs that growth cones encounter simultaneously as endogenous guidance cues interact with each other in determining the extent of growth cone turning. *2*) Normally, activation of neuronal nicotinic ACh receptors for example, by spontaneous, self-release of ACh, would enhance the turning effects of an endogenous EF, since inhibiting these receptors prevented cathodal turning. *3*) Activation of muscarinic or purinergic receptors would inhibit EF-induced turning since antagonists of these receptors enhanced cathodal turning. In addition, these findings suggest that spontaneous release of neurotransmitter by growth cones seeking out their targets could play a role in assisting pathfinding via an autoreceptor feedback mechanism (Fig. 17, *A* and *B*) (68).

Other interactions at the receptor level are central to EF-induced cathodal turning and indicate additional interactions between guidance cues. Spontaneous and evoked release of ACh increases rapidly and markedly on exposure of *Xenopus* embryonic neuromuscular synapses to the neurotrophins NT-3 and brain-derived neurotrophic factor (BDNF) (113). If these neurotrophins also enhance ACh release from growth cones and ACh receptor activation is essential for cathodal turning, then coexposure of growth cones to a physiological EF and either NT-3 or BDNF should enhance turning. It did (132). BDNF markedly increased the extent of growth cone attraction cathodally (3-fold at 150 mV/mm), and both BDNF and NT-3 reduced the EF threshold required for cathodal attraction. These events were mediated via specific activa-

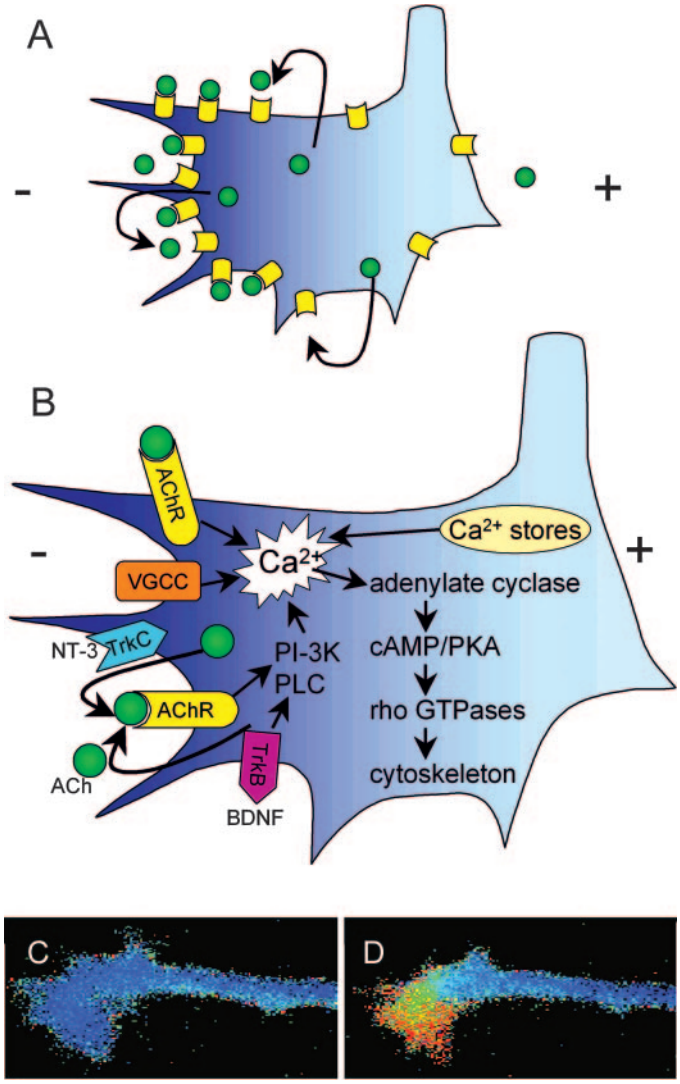

FIG. 17. Model for cathodal orientation of growth cones. *A*: membrane receptors accumulate preferentially toward the cathode-facing side of the growth cone (*left*). Candidate proteins include ACh receptors (AChR; yellow) because AChRs accumulate cathodally on cell bodies of EF-treated neurons, growth cones turn toward a source of ACh, and growth cones release ACh (green) spontaneously. ACh-induced stimulation of asymmetrically distributed AChRs activates signaling cascades preferentially on the cathode-facing side of the growth cone relative to the anode-facing side. This is reminiscent of the mechanism proposed to underlie turning of these same growth cones in a gradient of ACh. *B*: intracellular signaling cascades implicated in EF-induced cathodal turning (cathode to left). Cathodal turning requires influx of Ca^{2+} via voltage-gated Ca^{2+} channels (VGCC) and Ca^{2+} release from ryanodine and thapsigargin-sensitive intracellular stores. Activation of AChRs by spontaneous release of ACh induces cytoplasmic Ca^{2+} elevation further, since the receptors are "leaky" to Ca^{2+}. Activation of the trkC and trkB receptors is also required for cathodal turning. Addition of NT-3, the ligand for the trkC receptor (blue) or brain-derived neurotrophic factor (BDNF), the ligand for the trkB receptor (magenta) to the culture medium enhances the cathodal response. This implicates the AChR further because NT-3 and BDNF stimulate release of ACh from the growth cone, therefore enhancing the asymmetric signaling via AChRs at the cathodal side of the growth cone. trkB receptors and AChRs activate the phospholipase C (PLC), phosphatidylinositol 3-kinase (PI-3K) pathway, elevating intracellular Ca^{2+} even further. Ca^{2+} elevation stimulates cAMP production via adenylate cyclase. cAMP activates the protein kinase C-dependent kinase (PKA), which affects signaling by the rho family of small GTPases (rac1, rhoA, and cdc42). Activation of rac1 and cdc42 by PKA stimulate lamellipodial and filopodial formation, respectively. This is hypothesized to underlie the EF-stimulated orientation of filopodia and lamellipodia on the cathode-facing sides of growth cones, which are essential for cathodal orientation. Inhibition of rhoA by PKA activation cathodally prevents cathodal growth cone collapse, but relatively low levels of PKA signaling anodally permit rho-mediated growth cone collapse, further enhancing growth cone asymmetry. This leads to asymmetric tension within the growth cone and turning toward the cathode. Ca^{2+} elevation is central to the proposed mechanism. *C*: cytoplasmic Ca^{2+} levels are low in fura-loaded growth cones, but growth cone Ca^{2+} increases upon exposure to an EF of 150 mV/mm (*D*).

tion of trkB and trkC receptors, because the trk receptor antagonist K252a blocked the NT-3 effect and because neither nerve growth factor nor ciliary neuronotrophic factor (CNTF), which signal through other receptors, altered EF-induced cathodal attraction. Intriguingly, at a low EF strength of 10 mV/mm close to the threshold level for turning, NT-3 exposure switched the polarity of the turning response. Growth cones were repelled from the cathode and attracted anodally. Collectively these observations add the neurotrophin receptors trkB and trkC to the model outlined where EF-induced asymmetry of the neuronal nicotinic ACh receptor transduces the directional effects of the EF. It is not known whether the trkB and trkC receptors redistribute in an EF, but if they did BDNF and NT-3 would be expected to enhance ACh release more from one side of a field exposed growth cone than the other.

3. *EF-induced asymmetries of second messengers and cytoskeletal molecules?*

Pharmacological inhibitor experiments further indicate involvement of receptor tyrosine kinases, phospholipase C, several protein kinase C isoforms, extracellular Ca^{2+}, and Ca^{2+} from intracellular stores downstream from membrane receptor transduction of the EF into cathodal attraction (Fig. 17*B*) (128, 132, 192). In addition, there is direct evidence using fluorescent imaging of fura 2 and fluo 3 that an applied EF induces localized elevation in $[Ca^{2+}]$ in *Xenopus* (166) (Fig. 17, *C* and *D*) and *Helisoma* growth cones (45). In terms of the cytoskeleton acting as an effector of receptor and second messenger activation, growth cones treated with low doses of latrunculin (25 nM) or vinblastine (5 nM) showed diminished directional responses in an EF, indicating that functional microfilaments and microtubules, respectively, are important for cathodal attraction (165). Two of the small GTPases may link second messenger and cytoskeletal activation, since growth cones exposed to the bacterial toxins, toxin B (Fig. 15*C*), C3 transferase, or to a custom-designed peptide that inhibits cdc42 activity (200) did not show early cathodal attraction in 150 mV/mm (65). The emerging model (Fig. 17*B*) has major similarities to the pathways activated by the group I chemotropic guidance cues, which include ACh, BDNF, and netrin 1 (186). Modulating the levels of growth cone cAMP or cAMP-dependent kinases, such as protein kinase A (PKA), switches the growth cone response in the same gradient of ACh, BDNF, or netrin 1 from chemoattraction to chemorepulsion (188). This has resonance with our observation that in the presence of 100 ng/ml NT-3, a low EF strength converts cathodal attraction to repulsion (132). Clearly there is a need to monitor intracellular cAMP levels during EF-induced growth cone behaviors since this observation suggests that "low" and "high" physiological EFs could have opposing effects on [cAMP] in the growth cone.

Understanding of the mechanisms controlling the turning of growth cones in an EF clearly is incomplete. In particular, dynamic studies of receptor distribution, receptor activation, and second messenger activation, for example, of $[Ca^{2+}]_i$ and $[cAMP]_i$ at threshold levels of EFs are needed and would be timely given the realization that chemotaxis of lymphocytes and chemotropism of growth cones depend on receptors and signaling molecules that are probably drawn together in lipid rafts or signaling platforms (145, 161). It will be of interest to determine how an EF modulates the dynamics of signaling in these membrane microdomains, particularly in the light of recent indications that receptor asymmetry at the leading edge is not required for chemotaxis in *Dictyostelium* or in human neutrophils (49, 154, 208).

4. *Membrane protein electrophoresis or electroosmosis?*

The evidence that many receptor types accumulate cathodally on membranes of cells exposed to a physiological EF requires additional comment. First, since most integral membrane proteins are negatively charged, they would be expected to accumulate anodally if they were moved by electrophoresis. There is both theoretical and experimental evidence, however, to indicate that receptor rearrangements in an applied DC EF are driven by electrosmosis, which acts to override the effects of electrophoresis (135). Electrosmosis involves fluid flow within a layer only angstroms from the membrane surface. Na^+ and K^+ acting as counterions to the negatively charged membrane proteins accumulate, together with their associated water molecules, in this thin layer. Electrophoresis of these counterions induces a fluid movement and a hydrodynamic force that draws the negatively charged membrane proteins cathodally. Altering the balance of membrane negativity by adding positively charged lipids, such as DiI, or by removing negatively charged sialic acid residues from the membrane with neuraminidase shifts the balance of these forces such that negatively charged, fluorescently labeled membrane proteins then move electrophoretically and accumulate anodally (162). Second, there is the issue of the time taken to induce receptor asymmetries in cells and the relationship of this to the speed of the cellular responses which EF application induces. The electrophoretic mobility of membrane-embedded proteins in physiological EFs has been dealt with in detail (89, 92, 162). In short, receptor proteins such as the conA receptor become fully polarized in an applied EF of physiological magnitude within 10 min and are substantially asymmetric within 1–2 min (Fig. 16). This is entirely in keeping with receptor asymmetry being an initiating event in the transduction of the EF. It is important to

reiterate the issue of EF strength. It is often suggested that these EFs might orient extracellular elements such as collagen filaments. Jaffe (92) has calculated that it would require 4,000 V/cm to orient a 0.9-μm-long collagen filament. This is three to four orders of magnitude greater than the physiological EFs that induce such rapid and striking receptor rearrangements.

B. DC EFs May Be Pulsatile

In addition to the existence and physiological roles for steady DC EFs in development and in wound healing (above), there are many situations where external EFs arise from repetitive, pulsatile firing of action potentials, or from synaptic activity, particularly within the tight constraints of the extracellular spaces of the CNS (59). Importantly, pulsed DC EFs also induce cathodal attraction of *Xenopus* growth cones (157) and cathodal redistribution of conA receptors (215); therefore, the scope for extracellular EF effects in the CNS is considerable. This extends beyond influencing patterns of directed growth, since an applied EF as low as 1 mV/mm can synchronize and alter the action potential firing patterns of networks of neurons (66). This, in turn, may feedback to influence growth cone guidance. Brief periods of stimulation of cultured *Xenopus* spinal neurones caused a marked alteration in the turning responses of growth cones induced by gradients of attractive and repulsive guidance cues (141). Netrin-1-induced growth cone attraction was enhanced, and the repulsion induced by myelin-associated glycoprotein (MAG) was converted to attraction. As with the effects of steady DC EF application or gradients of chemotropic molecules alone, these effects appeared to be mediated by elevations of cytoplasmic Ca^{2+} and cAMP (141).

In terms of nerve chemotropism then, the level of intracellular electrical activity (action potential stimulation) alters the responsiveness of a growth cone to a given molecular gradient. Given that action potential stimulation, wounding, and developmental asymmetries in ion pumps and leaks all induce extracellular EFs within tissues, what consequences will this have for the formation or maintenance of chemical gradients? To establish that the cause of growth cone turning in an EF was a primary effect of the EF per se and not a secondary effect of the EF creating a chemical gradient in the culture dish, the point has been made already that growth cones responded quantitatively the same way to an EF in the presence of cross-perfused medium designed to disrupt standing chemical gradients. However, in vivo EFs establish chemical gradients. Injecting fluorescently labeled charged protein into the prelimb bud region of amphibian embryos, where large endogenous EFs have been measured, resulted not in a symmetrical diffusion of the marker, but in a comet tail-like distribution driven by extracellular electrophoresis of the fluorescent probe (138). Because EFs of this magnitude are present in many in vivo locations, it follows that wherever soluble charged molecules and EFs coexist in biology the influence of the EF to sustain or disrupt a standing chemical gradient must be considered.

C. Directed Cell Migration in a Physiological EF: Whole Cell Electrotaxis

Although the phenomenon of cells migrating directionally in a DC EF of physiological strength has been known for over a century (50), it is important to stress that this is not simply a matter of all cells migrating in the same direction. Cells derived from the same tissue can migrate in opposite directions. For example, corneal epithelial cells and osteoblasts migrate cathodally, and corneal stromal fibroblasts and osteoclasts migrate anodally (62, 189). At the same EF strengths, other cells such as human skin fibroblasts and melanocytes fail to migrate directionally (75, 182). In addition, the same cell type from slightly different locations, epithelial cells from the apex or from the equator of bovine lens, migrate in opposite directions in a physiological EF (205). Cell responsiveness to the endogenous EFs they encounter in development and in regeneration therefore is likely to involve complexities and subtleties that are only beginning to be recognized. A comprehensive review of vertebrate cell types and their migratory behavior in an applied EF is available (149). Here we concentrate on selected cell types where some mechanistic detail is available to do two things: *1*) compare and contrast the mechanisms underpinning EF-directed migration and cell chemotaxis and *2*) compare and contrast the mechanisms driving cell electrotaxis with those outlined above for nerve growth cone electrotropism (Fig. 18 and Table 1).

1. The cornea as a model system

Corneal epithelial cells (CECs) are useful in studying electrotaxis because wounds in corneal epithelium generate an endogenous EF that controls the rate of reepithelialization (184), by regulating both cell migration and cell division (Figs. 9 and 10). Multiple levels of analysis are possible, and we have used dissociated single cells (see movie 2, which is located at http://physrev.physiology.org/cgi/content/full/00020.2004/DC1) (217), scratch wounds in monolayer cultures, excised organ culture of whole cornea (223), and in vivo rat corneal wounds (184) to ask different questions. Single CECs migrate cathodally, and some elements of the pathway underlying this are known (Table 1). In serum-free medium, bovine CECs continue to migrate, but they lose all directionality with respect to the EF vector (217). Adding EGF, bFGF, or transforming growth factor (TGF)-β1 to serum-free cul-

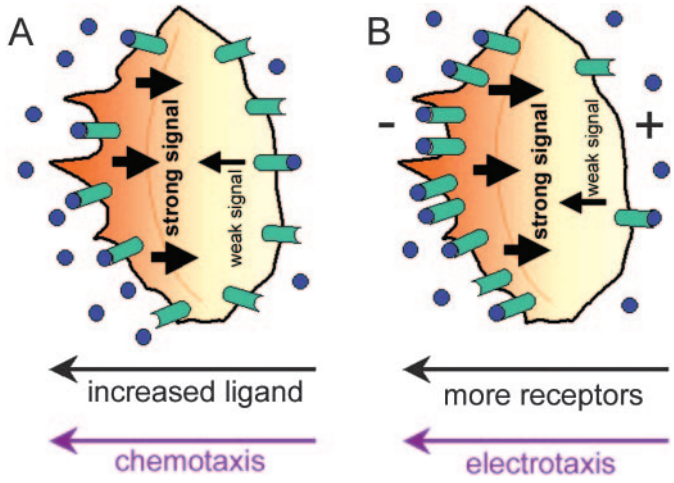

FIG. 18. Model proposed for chemotaxis (*A*) and electrotaxis (*B*) of epithelial cells. *A*: in chemotaxis a gradient of ligand stimulates activation of more receptors on one side of the cell than the other. The result is increased cytoplasmic signaling on one side of the cell relative to the other, even if the receptor density is the same on each side. The side of the cell with higher signaling becomes the leading edge, and the cell migrates up the ligand gradient. *B*: in electrotaxis, asymmetric signaling results from an increase in density of membrane receptors (or membrane) on the cathode-facing side of the cell. The intracellular signal is higher on the cathode-facing side of the cell, which becomes the leading edge, and the cell migrates toward the cathode.

ture medium restored directed migration partially, in a dose-dependent manner, and in combination the three growth factors added to serum-free medium restored cathodal migration fully. Several growth factor receptors therefore may act together perhaps using parallel signaling pathways to transduce the effects of an EF. Most work has concentrated on EGF, because wound healing in the cornea involves upregulation of EGF and requires activation of EGF receptors at the leading edge (226). Importantly, this is the region in the cornea where the wound-induced DC EF is strongest (see Fig. 7). Flow cytometry shows that applying an EF upregulated EGF receptors (EGFRs) and caused redistribution of EGFRs and of F-actin towards the cathodal side of CECs in <10 min. In serum-free medium in which cathodal-directed migration fails, upregulation of EGFRs and cathodal accumulation of EGFR and F-actin also did not occur (219).

Cathodal accumulation of EGFRs and of membrane surface area as assessed with the fluorescent membrane lipid dye DiI were identical quantitatively (222). This suggests that membrane area increased cathodally because of membrane folding. Therefore, although functionally there would be more receptors available to be activated at the cathodal leading edge, the concentration of receptors per unit area may not have increased. A similar situation appears to underpin neutrophil chemotaxis (177). Cathodal accumulation of F-actin microfilaments was a consequence of receptor and membrane asymmetries rather than a cause, because asymmetries of both EGFR and DiI persisted in the presence of 0.5 μM latrunculin, which inhibits actin polymerization. EF-induced asymmetry of EGFRs also induced asymmetric intracellular signaling through the mitogen-activated protein (MAP) kinase signaling cascade. Western blots showed increased activa-

TABLE 1. *Molecules underpinning directional migration in chemical and electrical gradients*

Molecular Target	Neuronal Growth Cones		Nonneuronal Cells	
	Chemotropism	Electrotropism	Chemotaxis	Electrotaxis
EGFR	ND	ND	Yes (7)	Yes (219)
VEGFR	ND	ND	Yes (4)	Yes (218)
FGFR	Yes (206)	Yes (57)	Yes (104)	Yes (217)
G proteins	Yes (76, 212)	ND	Yes (37, 48, 169)	No (221)
PKC	Yes (69)	Yes (58)	Yes (199)	Yes (150), no (164)
PLC	Yes (76, 140)	Yes (58)	Yes (111, 211)	ND
PI-3K	Yes (111)	ND	Yes (40, 169)	Yes (218)
IP_3	Yes (76)	Yes (58)	Yes (146)	ND
Ca^{2+}	Yes (142)	Yes (58, 192), no (153)	Yes (105, 155)	Yes (60, 152, 196), no (30)
cAMP/PKA	Yes (80, 114, 188)	Yes (124, 153)	Yes (54, 151)	Yes (150, 164)
Rho GTPases (rac1, rho A, cdc42)	Yes (195, 216)	Yes (65)	Yes (190, 207, 213)	ND
MAPK/ERK1/2	Yes (155)	ND	Yes (97, 137)	Yes (219)
Protein synthesis	Yes (33, 155)	ND	Yes (181)	ND
AChR	Yes (188)	Yes (57)	Yes (110)	ND
BDNF/Trk B	Yes (188)	Yes (132)	No (101)	ND
Netrin-1/DCC	Yes (111)	ND	Yes (112)	ND
NGF/Trk A	Yes (52, 111)	No (132)	Yes (101)	ND
NT-3/Trk C	Yes (188)	Yes (132)	Yes (101)	ND

ND, not determined; EGFR, epidermal growth factor receptor; VEGF, vascular endothelial growth factor receptor; FGFR, fibroblast growth factor receptor; PKC, protein kinase C; PLC, phospholipase C; PI-3K, phosphatidylinositol 3-kinase; IP_3, inositol 1,4,5-trisphosphate; PKA, cAMP-dependent protein kinase A; MAPK, mitogen-activated protein kinase; ERK1/2, extracellular signal-related protein kinase; AChR, acetylcholine receptor; BDNF, brain-derived neurotrophic factor; Trk B, tyrosine kinase receptor type B; DCC, deleted in colorectal carcinoma; NGF, nerve growth factor; Trk A, tyrosine kinase receptor type A; NT-3, neurotrophin-3.

tion of dual phosphorylated ERK1/2, which immunohistochemically was predominant cathodally. In addition, activated ERK1/2 and F-actin became highly colocalized at the leading lamellae of CECs migrating cathodally (Fig. 19) (222).

The phosphatidylinositol (PI) 3-kinase inhibitor LY294002 and the MAP kinase inhibitor U0126 both reduced, but did not abolish, cathodal-directed migration, indicating the involvement of more than one signaling pathway.

In short, the mechanism driving EF-directed CEC migration and EF-directed growth cone turning share several elements in common. Each can be transduced by an induced asymmetry of membrane receptors known to operate also in transducing the response to a locally relevant chemical gradient. Each involves signal transmission at the leading edge by second messenger pathways also used to respond to chemical gradients, and each is affected by asymmetric activation of F-actin. Figure 18 and Table 1 compare and contrast the mechanisms that control electrically and chemically directed cell movements in epithelia and in neuronal growth cones.

2. Electrical control of lens epithelium

The vertebrate lens drives electrical current through itself (Fig. 20). Lens epithelial cells (LECs) are present in a hemispherical cap on the anterior surface of the lens. The basal surface of these cells abuts the lens capsule, and basolateral Na^+-K^+-ATPase activity results in high internal K^+ within the extracellular spaces of the lens and high Na^+ outside. Using a vibrating microprobe, currents of 20–40 $\mu A/cm^2$ have been measured flowing out of the lens equator and returning across the anterior surface (174) (Fig. 20). The use of published values for equatorial and polar lens resistivity of 0.5 and 500 kΩ/cm indicates that lens currents will give rise to steady DC EFs of between 2 and 600 mV/mm, a normal physiological range. Current flow draws associated water through the avascular lens, and this may flush out metabolites (116). Intriguingly, current efflux is concentrated at the lens equator where important aspects of lens physiology take place. Throughout adult life, lens epithelial cells move towards the equator, probably by active migration, proliferate in organized parallel arrays here, elongate, and transdifferentiate into lens fiber cells. The latter become compacted and lose their internal organelles to form the transparent interior of the lens. The factors regulating these key developmental events include FGF, which promotes migration, proliferation, and differentiation in a dose-dependent manner (118). The formation of an anterior-posterior gradient of bFGF and increasing expression of FGF receptor subtypes on cells nearing the equator are key elements in this control. Mimicking the natural electrical signals of the lens equator by applying a physiological EF to LEC in culture induces many of the cellular events that occur near the equator. An EF directed LEC migration, promoted cell elongation and cell reorientation (205, 204), and regulated cell cycle progression to mitosis (201). EF-directed cell migration was serum dependent, and directed migration was restored partially by adding bFGF to serum-free medium. This indicates that the FGF receptors are required for this response, but we have been unable to demonstrate any EF-induced receptor asymmetry in single cells. Interestingly, the direction of cell mi-

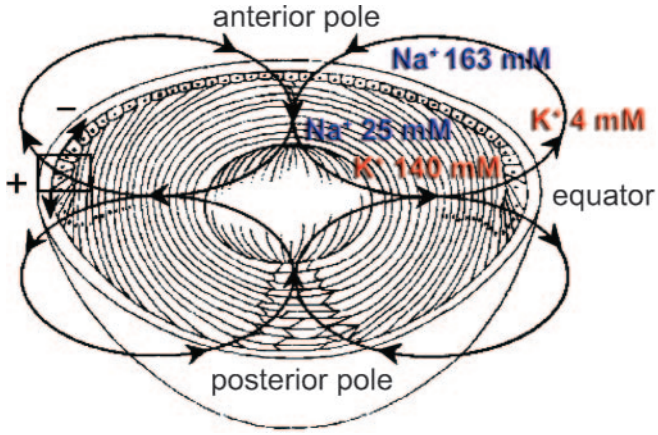

FIG. 20. Diagram illustrating endogenous EFs in the lens and potential effects of the EFs on LEC behavior. Current flows outward at the equator and returns inward at both poles of the vertebrate lens. These current loops create physiological EFs within the lens. Currents are generated by Na^+-K^+-ATPase pumps in the basolateral membranes of anterior epithelia. Thus K^+ accumulates in the lens interior, and Na^+ accumulates out with the anterior pole, while both aqueous humour and vitreous contain low K^+ and high Na^+. These respective chemical gradients drive the current loops, with K^+ driving current out at the equator and Na^+ driving the return current loops in at the anterior pole (see Refs. 116, 118). LEC proliferation, migration, and reorientation occur from a germinative zone immediately above the lens equator (box at *left*). LECs migrate either towards the equator, elongate, and transdifferentiate, to become lens fiber cells, or they migrate towards the front of the lens, to compensate for ongoing apoptosis of LECs, as the epithelium turns over. Many of these cell behaviors, including bidirectional migration of equatorial cells, are mimicked by culturing LECs in a physiological EF. The role of the endogenous EF remains to be determined.

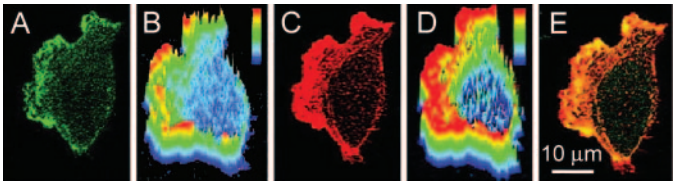

FIG. 19. Asymmetry of dp-ERK (activated mitogen-activated protein kinase) (*A* and *B*) and F-actin (*C* and *D*) in corneal epithelial cells exposed to physiological electric fields. *A*: in an EF of 150 mV/mm, ERK (green) was activated preferentially at the cathodal side, together with accumulation of F-actin (red, *C*), and they were colocalized (*E*). *B* and *D*: surface plots of *A* and *C*, respectively. Fluorescent intensity is indicated from strongest to weakest by red gradually changing from red to blue, which illustrates activation of ERK and accumulation of F-actin at the leading, cathodal-facing side of the cell.

gration depended on both EF strength and on the origin of the cells. LECs from the anterior and equatorial lens migrated anodally at 150–250 mV/mm. At 50 mV/mm however, LECs from the equator migrated in the opposite direction, cathodally, but anterior LECs did not respond. These data indicate *1*) that only equatorial LECs showed EF strength-dependent bidirectional migration and *2*) that cells of the same type but from slightly different locations respond differentially to an EF and at different thresholds. As with corneal epithelial cells, the MAP kinase signaling pathway was involved in EF-directed migration. EF-directed migration was lost in cells treated with U0126, a MAP kinase inhibitor. In addition, an EF enhanced the expression of active ERK1/2, a signaling enzyme in the MAP kinase pathway, at both 50 and 200 mV/mm, field strengths which stimulated migration in opposite directions. Anterior LECs, which did not migrate directionally at 50 mV/mm, did not show enhanced ERK1/2 at this EF strength, but did at 200 mV/mm, which stimulated anodal migration. Both enhanced ERK1/2 expression and directed migration required serum (205).

Irrespective of the significance of this phenomenology in normal lens development, a role for EFs in controlling LEC behavior has clinical potential. Millions of cataract patients have their lens removed and a synthetic replacement inserted in the capsular bag. A frequent complication involves proliferation and migration of residual lens epithelial cells over the posterior part of the lens capsule (an area they are excluded from normally) and over the new lens. Perhaps this aberrant LEC behavior arises because the normally present electrical control is removed when the lens is excised. This produces posterior capsule opacification, serious visual acuity problems, and needs to be corrected with expensive laser surgery. Finding new ways to control aberrant migration and proliferation of LECs therefore is important. We have shown using scratch wounds in monolayers of LECs that the wound edge facing the anode heals by closing, but the edge facing the cathode fails to heal and opens up (over 2 h) (203). In addition, proliferation of LECs was suppressed markedly over 24–48 h. Both flow cytometry and Western blotting indicate that this occurs because the EF regulates levels of key cell cycle control enzymes. Levels of expression of the G_1 specific cyclin, cyclin E were suppressed whilst the cyclin-cdk complex inhibitor $p27^{kip1}$ was enhanced thus restricting G_1 to S phase transition (Fig. 21) (201). The same pattern of suppressed proliferation through EF regulation of the cell cycle has been seen in vascular endothelial cells (202). Restraining LEC proliferation and migration electrically would be a novel and promising approach to the problem of posterior capsule opacity.

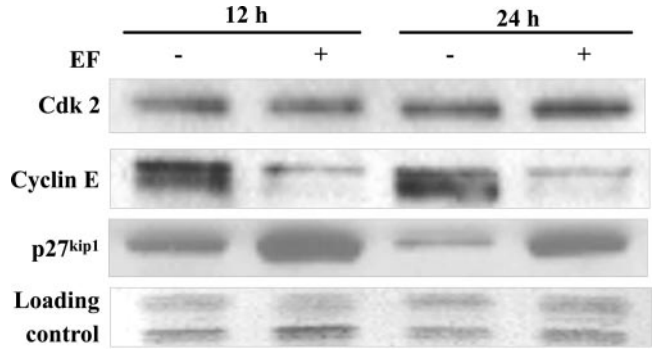

FIG. 21. Western blotting analysis for the expression of cyclin E, Cdk2, and $p27^{kip1}$ in a human LEC line. At 12 and 24 h after EF exposure, respectively, the cells were rinsed briefly with PBS and lysed. Identical amounts of protein lysates were resolved by SDS-PAGE, followed by electroblotting onto nitrocellulose membranes. The membranes were probed with anti-cyclin E, anti-Cdk2, and anti-$p27^{kip1}$ antibodies, respectively. The gel containing proteins was stained with Coomassie Blue as a loading control. EF exposure downregulated the expression of cyclin E and upregulated the expression of cyclin E/Cdk inhibitor $p27^{kip1}$, but did not influence the expression of Cdk 2. [From Wang (201).]

3. Electrical control of vascular endothelium

Applying a physiological EF also induces a striking reorientation of some cells. Myoblasts and endothelial cells, for example, form or realign their long axis to lie perpendicular to the EF vector (78, 218). In a sheet of vascular endothelial cells this is a striking phenomenon (Fig. 22*B*). A sheet of cobblestone-like endothelial cells is transformed to resemble the inner surface of a blood vessel, comprising highly ordered and highly elongated cells (compare Fig. 22, *A* and *B*). Some aspects of the mechanisms controlling this are known. Vascular endothelial cells exposed to an EF in culture increase secretion of the angiogenesis producing growth factor vascular endothelial growth factor (VEGF). Secretion increases severalfold within 5 min, peaks around 30 min before dropping off, and undergoes a second peak in VEGF release between 4 and 24 h. Cells exposed to the VEGFR1 and R2 inhibitor 4,4′-(chloro-2′-fluoro)phenylamino-6,7-dimethoxyquinazoline fail to reorient perpendicular to a physiological EF, indicating that self-release of the ligand VEGF and activation of VEGFR1 are primary elements in the transduction of this response. VEGFR activation is signaled through the PI 3-kinase/Akt/rho kinase pathway, and significantly perpendicular reorientation of endothelial cells was inhibited partially by the PI 3-kinase inhibitor by LY294002, an Akt inhibitor (serine/threonine kinase inhibitor), and by the rho kinase inhibitor Y27632. A similarly striking reorganization of a sheet of endothelium takes place in response to shear stress by realignment of the long axes of endothelial cells in the direction of fluid flow. This is mediated by the $\alpha_v\beta_3$-integrin. EF-induced perpendicular cell reorientation however must be driven by different mechanisms, since functional blocking antibodies to $\alpha_v\beta_3$ did not prevent this (218).

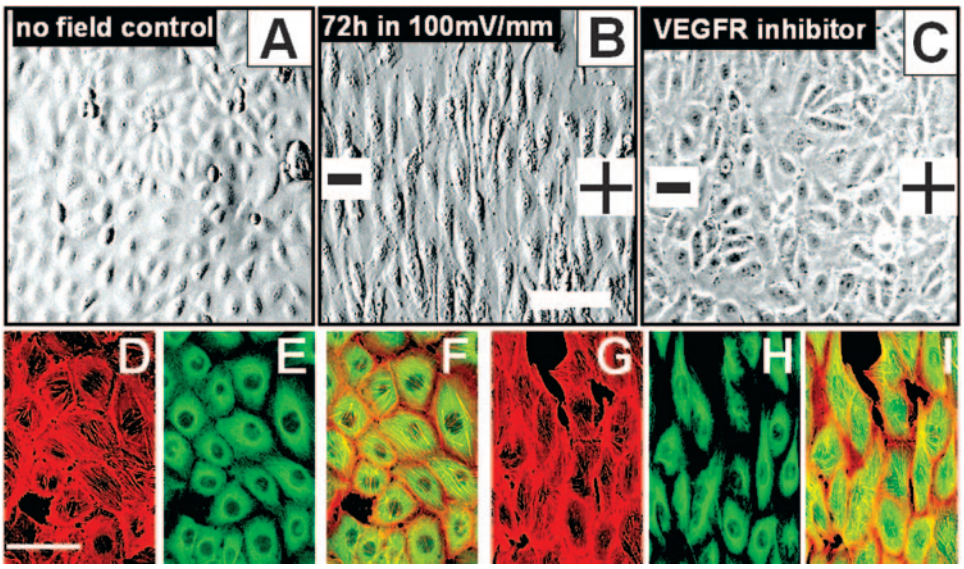

FIG. 22. Perpendicular orientation and elongation of endothelial cells in a small physiological EF. *A*: control HUVECs cultured without an EF showed a typical cobblestone morphology and random orientation. *B*: cells exposed to small-applied EF showed dramatic elongation and perpendicular orientation in the EF. *C*: cells treated with a VEGFR inhibitor completely abolished perpendicular orientation and significantly inhibited elongation in an applied EF (72 h; 100 mV/mm). *G* and *H*: the majority of actin filaments (red) and microtubules (green) became aligned along the long axis of the cells (12 h at 150 mV/mm). *D*, *E*, and *F*: no field controls showed no obvious alignment and cell elongation. *F* and *I*: merged images. *Image C* is a phase-contrast image, but *A* and *B* were taken using Hoffman modulation optics. [From Zhao et al. (218).]

In addition to reorienting endothelial cells, an applied EF also stimulated cell migration, anodally, and cell elongation. Human umbilical vein endothelial cells (HUVEC) cultured for 24 h were twice as long as they were broad (no EF). In an EF strength-dependent manner and with a threshold between 50 and 75 mV/mm, an applied EF nearly doubled the long-to-short axis ratio to 3.5 at 300 mV/mm (24 h). The drugs that inhibited EF-induced reorientation also inhibited EF-stimulated elongation, indicating a commonality of receptor and second messenger mechanisms.

These three cell behaviors, reorientation, elongation, and directed migration, are all forerunners of angiogenesis. Each is regulated by a physiological EF, and angiogenesis frequently takes place within a steady EF; vascular sprouting directed towards a wound (32) and towards tumors (44) are two examples. Endogenous EFs therefore may regulate angiogenesis in vivo. It may also be worth testing the notion of using an applied EF to direct blood vessel growth in vivo, for example, to prevent new blood vessels from entering tumors.

4. *Directional migration of Dictyostelium discoideum in electric fields*

In the context of comparing and contrasting the mechanisms underpinning chemotaxis and electrotaxis, the social amoebae *Dictyostelium discoideum* is a powerful model system. This is because, although these amoebae would not naturally encounter a DC EF, they are amenable to both genetic (its genome sequence is nearly complete) and biochemical analyses (103), much is known already regarding the signaling events that regulate chemotaxis, and they show strong electrotaxis. *D. discoideum* grow as single cells, but upon starvation they enter a developmental program where individual cells undergo chemotaxis to form multicellular aggregation centers (6, 49, 98). The most potent chemoattractant for *D. discoideum* is cAMP, which is secreted endogenously and directs aggregation via a specific family of seven transmembrane receptors, the cAMP receptors (cARs), a group of heterotrimeric G protein-coupled receptors. In chemotaxis, G protein-coupled receptors sense chemoattractants and regulate pseudopod extension at the leading edge (37). We have investigated whether electrotaxis and chemotaxis share signaling mechanisms through G protein-coupled receptors. We have shown that the early stages of signal reception and transduction are not shared, but that the respective signaling strategies converge somewhere upstream of directed F-actin polymerization. When exposed to a relatively high DC electric fields of 700 mV/mm, *Dictyostelium* cells show very strong directional migration, and at 1,500 mV/mm virtually all cells moved in straight lines towards the cathode (221) (http://www.jcb.org/cgi/content/full/jcb.200112070/DC1/5).

Dictyostelium cells that enter the development stage use G protein-coupled receptor signaling to direct chemotactic migration to a source of cAMP. The most important receptor for this is cAR1. cAR1−/cAR3− cells (RI9) were used to test whether cAMP receptors were involved in electrotaxis. These cells, which show no chemotaxis towards cAMP, maintained significant directional migration toward the cathode in DC EFs (http://www.jcb.org/cgi/content/full/jcb.200112070/DC1/6). The $G_2\alpha$ subunit together with the $G\beta\gamma$ complex couple with cAR1 and transduce cAMP-binding into various responses. Like cAR1/cAR3-null mutants, $G_2\alpha-$ cells (MYC2) also maintained directional migration in an EF (http://www.jcb.org/cgi/content/full/jcb.200112070/DC1/7). The $G\beta\gamma$ subunit is essential for chemotaxis to all chemoattractants (96), and interestingly, di-

rectional migration of Gβ− cells in an EF was reduced by about one-half compared with wild-type cells (221) (http://www.jcb.org/cgi/content/full/jcb.200112070/DC1/8).

Asymmetry in signaling drives the polarized actin changes needed for directed lamellipodium or pseudopodium extension during chemotaxis (37, 227). Membrane recruitment of the PH domain-containing protein CRAC (cytosolic regulator of adenylate cyclase, PHcrac) is an indicator of G protein signaling, and the use of GFP fusion constructs in *Dictyostelium* (PHcrac-GFP) and neutrophils (PHAkt-GFP) has shown that phosphatidylinositol 3,4,5-trisphosphate and phosphatidylinositol 3,4-bisphosphate generated upon activation of the G protein-coupled receptors are polarized toward the chemoattractant source (136, 176). Spatial regulation of PI 3-kinase and phosphatase activities therefore are crucial for directional sensing during G protein-mediated chemotaxis (169, 40). In wild-type cells expressing PHcrac-GFP, there was no redistribution of PHcrac-GFP during electrotaxis or after polarity reversal (http://www.jcb.org/cgi/content/full/jcb.200112070/DC1/10), indicating that the EF did not act upon the G protein subunits or their immediate effectors to direct movement.

Membrane receptor redistribution may be involved in cell responses to EFs and has been demonstrated in several cell types (30, 61, 163, 219). Cathodally directed migration of corneal epithelial cells involved induced asymmetry of membrane lipids and associated EGF receptors and asymmetric activation of MAP kinase signaling shown by leading edge asymmetry of dual phosphorylated extracellular signal-regulated kinase (222). Using cAR1-GFP-expressing cells, we monitored the dynamic distribution of receptors during electrotaxis in *Dictyostelium*. Neither obvious redistribution nor accumulation at the leading edge was observed during electrotaxis or during field polarity reversal (http://www.jcb.org/cgi/content/full/jcb.200112070/DC1/9). Therefore, EF-induced receptor asymmetry is a selective event, and not all receptor types are redistributed by an EF. Whether and in what direction individual receptor molecules are moved by an applied EF will depend in part on the balance between the charge carried by the receptor and that on the membrane surface.

Actin was polymerized at the leading edge in electrotactic cells (221). Coronin is an actin binding protein important for actin reorganization in *Dictyostelium* (72), and coronin-GFP marks regions of intense actin polymerization. We monitored the dynamic distribution of this construct in both wild-type and β− cells. Coronin-GFP accumulated at the leading edge in both cell types and reversed to the other end when the EF polarity was reversed (http://www.jcb.org/cgi/content/full/jcb.200112070/DC1/11, http://www.jcb.org/cgi/content/full/jcb.200112070/DC1/12). Similar proportions of cells showed cathodal redistribution of coronin-GFP in both AX3 and β2 cells. This suggests that although the Gβ subunit may contribute to electrotaxis (directionality data), when this was nullified, substantial asymmetry of F-actin still developed to drive electrotaxis. How the EF directs actin polymerization remains to be elucidated.

Therefore, with the exception of partial dependency on the Gβ subunit, electrotaxis in *Dictyostelium* does not use the signaling elements that underpin chemotaxis. Thus reception and transduction of the electrotaxis signal are largely independent of G protein-coupled receptor signaling and the pathways driving chemotaxis and electrotaxis only come together downstream of heterotrimeric G proteins to invoke polarized cytoskeletal polymerization. The receptors and signaling molecules that initiate, transduce, and effect electrotaxis in *Dictyostelium* remain unknown. This lack of shared mechanisms between chemotaxis and electrotaxis in *Dictyostelium* is intriguing given the strong parallels between electrotropism and chemotropism of *Xenopus* neuronal growth cones and electrotaxis and chemotaxis of corneal epithelial cells (Table 1 and Fig. 18).

D. Electrical Control of Wound Healing and Tissue Regeneration

The endogenous EF at a corneal wound stimulates and directs epithelial cell proliferation and cell migration at a wound edge and in this way promotes wound healing (see above) (184). To explore this further, we have developed a monolayer scratch wound model and an excised whole corneal preparation (184, 223). These model systems allow study of the interplay between the influences that control wound healing. Wounding an epithelium (either the whole tissue or a monolayer) causes release of growth factors and cytokines, particularly at the wound edge (38). Although there is no direct demonstration that a chemical gradient of these molecules is established, this is widely assumed to occur and to be the primary driver of wound healing. The presence of a free wound edge also may stimulate cell migration to close the wound, because cells at the leading edge are released from contact inhibition. We have mimicked the situation in vivo by testing the effects of simultaneously applying a physiological DC EF to these models in which chemical gradients and the freed wound edge are assumed to control wound healing. Surprisingly, in corneal epithelial monolayer wounds and wounds in excised whole cornea, the polarity of the EF determined whether a wound closed or opened up. A wound edge facing the cathode healed faster than with no EF, as has been shown previously in vivo (184, 191). Remarkably, however, wounds facing anodally not only failed to close, but they opened up. It must be stressed that the normal cues thought to control wound closure, chemical gradients and the presence of a free wound edge, are present in these cases. All that has been added

is an applied EF of a strength equivalent to that measured at skin and corneal wounds but with a normal (wound cathode) or reversed polarity (wound anode). These observations allow several conclusions. *1*) They show that the cues thought to control wound healing, chemical gradients and the removal of contact inhibition, are not sufficient to close a wound. *2*) An EF together with normal sources of chemical gradients and a free wound edge enhance healing. *3*) An EF can override and dominate the healing influences of normal sources of chemical gradients and of a free wound edge. One interpretation of this is that a physiological EF is at the head of a hierarchy of cues that interact to promote wound healing.

Applied EFs with a wide variety of stimulation protocols have been used clinically to treat nonhealing skin wounds (71). Many studies have claimed success, and this disparate literature is reviewed comprehensively elsewhere (149, 197). It is riddled with poor and uncontrolled experiments in which various types of metal electrodes have been inserted directly into a wound bed. In these cases, the secondary electrochemical effects of metal ions, or of O_2 or H^+ released by the electrodes, which will change the tissue pH in the wound, have not been separated from the primary effects of the EF alone. Unfortunately, clinical practice has proceeded ahead of our understanding of the cell biology of EF-directed wound healing and therefore has not been best informed. The optimal stimulation protocol to treat human skin wounds with an applied DC EF will be determined only when the cell biology is understood in greater detail.

Nevertheless, there is one intriguing case of wound healing in humans that is associated with injury currents. Adolescent humans regenerate an amputated fingertip fully from the distal phalange including the nail, but only if the wound stump is dressed and left open and hydrated. If the wound is sutured together and dries up, the fingertip does not regenerate. Interestingly, currents of 30 $\mu A/cm^2$ have been measured leaving such wounds. One interpretation of these observations is that dressing the wound and leaving it moist allows continued electrical conduction through the wound which contributes to regeneration (85), whilst suturing the wound closed diminishes electrical conduction and therefore prevents regeneration.

E. Electrical Fields and Cancer?

One further area in which DC electrical signals may play a role is in the control and spread of cancer cells. Transformed cells are perturbed electrically. They have a greater negative surface charge than normal cells, and usually their membrane potential is depolarized markedly (3, 12). In addition, the TEP of the skin of normal and transformed breast epithelium differs, and this is used clinically to diagnose the early onset of breast cancer in women (44). There are reports also of small steady extracellular voltage gradients between cancerous tissue and neighboring normal tissue, which could act as guidance cues promoting and directing cancer cell migration (144). Interestingly, a highly metastatic rat prostate cancer cell line responded strongly to an applied DC EF by migrating towards the cathode. In contrast, a weakly metastatic cell line did not respond at similar EF strengths. Cathodal-directed migration was blocked with tetrodotoxin, indicating the involvement of voltage-gated sodium channels in EF-directed migration of the highly metastatic cell line (51).

Despite this limited background knowledge, sporadic attempts have been made to treat easily accessible tumors with electrical stimulation often using a DC EF generated from an indwelling electrode (148). Although some successes are claimed, much too little is known about how cancer cells respond in culture or in vivo to this type of stimulation to know what is being done using this type of intervention. The point needs to be made again. Different cell types show subtly different responses to a DC EF. Among other influences, their response depends on EF strength, which will vary with variable local tissue resistances, the polarity of the EF, the extracellular matrix composition, the coexistence of certain growth factors or neurotransmitters, and the level of second messenger molecules within cells.

VI. CLINICAL UTILITY: ELECTRICAL CONTROL OF REGENERATION IN THE CENTRAL NERVOUS SYSTEM

In the historical introduction to this review, the seminal work of Borgens et al. (24) in testing a role for endogenous injury potentials in controlling axonal regeneration in the CNS was raised. They showed that intense injury currents of up to 100 $\mu A/cm^2$ carried by Na^+ and Ca^{2+} were driven into the cut ends of severed Muller and Mauthner axons of the lamprey spinal cord (Fig. 1*B*) (22). By passing current that established a steady DC EF of opposite polarity to the injury potential, they showed that this induced increased branching and faster regeneration of these naturally regenerating axons. This principle of using an applied DC EF to stimulate and direct axon regeneration has been extended to the currently intractable problem of promoting mammalian spinal cord repair. The cutaneous trunci muscle reflex in guinea pig is the equivalent of the reflex that cattle use to remove flies from the skin on their back, the sensory stimulus causing the subdermal musculature to twitch. Borgens and colleagues (18–20) have used the well-recognized neuroanatomy of this reflex in ground-breaking studies on the effects of applying a DC EF to the hemisected guinea pig spinal

cord. An EF of ~400 μV/mm was imposed across the hemisection for ~3 wk, with the cathode placed rostral to the transection plane since only the long ascending sensory nerve tracts within the dorsolateral white matter were assessed histologically. The original plane of transection was marked with an indwelling staple-shaped device (Fig. 23, *A* and *B*). Sham-treated animals showed no axonal regeneration and no return of the reflex. Fluorescently labeled axons died back by ~100–300 μm, and labeled terminals were rarely present within the lesion scar at 3 mo. In electrically treated spinal cords, a few labeled axons were traced around the lateral margins of the lesion and through undamaged spinal cord into the rostral segment. No evidence of branching was seen in the long tracts of the caudal cord. The traced axons therefore were singular extensions of axons of the severed dorsal and dorsolateral ascending columns. This is important work, since it shows that axons in adult mammalian spinal cord were stimulated electrically to regenerate around the margins of the lesion and to project into and through the fibroglial scar at the lesion site (Fig. 23, *C* and *D*). Despite the significance of this, only a small proportion of fibers was marked with dye injection, and very few nerves penetrated the transection site. Borgens (15) has used a different approach to demonstrate that an applied EF stimulates and directs regenerative growth of large numbers of myelinated axons in damaged spinal cord. A hollow silicone tube (6 mm × 1 mm) containing an electrode was implanted into a longitudinal slit in the dorsal spinal cord of adult guinea pig. With no current passing, virtually no regenerating fibers had entered the tube after 1–2 mo. This is as expected, since adult mammalian spinal cord axons normally do not regenerate. When the electrode was a cathode, however, massive regenerative axonal growth was stimulated, attracted to enter and to grow through the 6-mm length of the tube. This study established therefore that an applied EF *1*) stimulated robust regeneration of nerves within the adult mammalian spinal cord and *2*) that growth of these regenerating fibers was guided towards the cathode. A direct demonstration of the repellent effect of anodal current in vivo was not possible because when the implanted electrode was an anode, the buildup of electrode products trapped within the nonpermeable silicone tubes was toxic to the local tissues (15).

Restoring some function following spinal cord transection also has been achieved using stimulation with an applied DC EF. In adult guinea pigs a complete transection of the right side of the spinal cord permanently eliminates the cutaneous trunci muscle (CTM) reflex on that side, because of a failure of ascending CTM nerve tracts to regenerate. The reflex on the contralateral side remains normal and acts as a control. Passing 35 μA of DC current across the hemisected dorsal cord for 4 wk established an EF of ~300–400 μV/mm (cathode rostral) and induced variable levels of behavioral recovery of the CTM reflex in 25% of adult guinea pigs. With the anode rostral to the lesion, or when treatment was delayed for 3 mo after spinal cord hemisection, behavioral recovery did not occur (17, 23). Behavioral recovery was associated

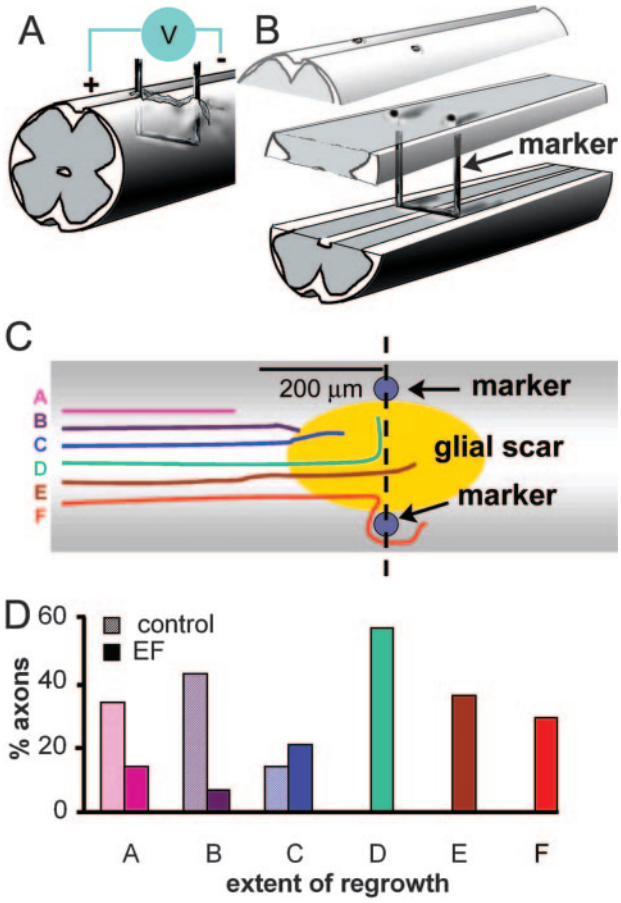

FIG. 23. An electric field stimulates regrowth of axons in the adult spinal cord. *A*: a dorsal hemisection was made in the guinea pig spinal cord. A miniature voltage source was implanted under the skin with wires leading to electrodes placed on the surface of the spinal cord, with the cathode rostral and the anode caudal to the lesion. A staple-shaped metal marker was inserted into the lesion at the time of surgery and it remained in place throughout the experiment. *B*: the marker was removed when the spinal cord was processed for histological examination. Longitudinal sections were made so the trajectories of labeled neurons could be traced. The holes left in the tissue by the marker meant that the lesion site could be determined reliably in all sections. *C*: a view through a section of the spinal cord similar to the middle slice in *B*. The holes left by the marker device are shown as circles at the edge of the cord. A glial scar forms at the lesion site. Regenerating axons were categorized according to the extent of regrowth: *A*, tip of axon >200 μm from the plane of transection; *B*, tip of axon <200 μm from transection plane; *C*, axon penetrates the glial scar; *D*, grew to the plane of the lesion; *E*, axon grew through the lesion; *F*, axon grew around the lesion. *D*: quantitative analysis of regrowth in animals without any applied EF ($n = 14$) and an EF ($n = 14$). In the absence of an EF, no axons reached to or beyond the lesion site, but EF-treated animals showed a significant increase in those categories. Most axons (57%) reached the lesion site, 36% could be traced through the lesion, and 29% grew around the lesion. [Redrawn from Borgens (13).]

with regeneration of axons in the ventrolateral spinal cord which carries CTM fiber tracts.

Collectively, this work indicates that spinal axon regeneration and the functional recovery of a specific spinal reflex may be promoted by a DC EF. However, both ascending and descending axon tracts are damaged in spinal cord injuries, and culture studies show that DC EFs of opposite polarity have opposing effects: the cathode stimulates and attracts nerve growth, the anode causes repulsion or retraction. However, cathodal attraction of growth cones in culture occurs within minutes, whereas anodal repulsion is slower to develop and retraction is not obvious until ~45 min (121). This asymmetry in response time offers the possibility of alternating the polarity of the EF every 30 min or so to attract axons in one direction while causing minimal retraction of those projecting in the "wrong" direction. Repeated switching of EF polarity would promote growth of axons projecting in opposing directions because there would be minimal time for retraction to occur in both directions (121). This principle of exposing spinal neurons to oscillating DC EF stimulation has been tested using spinal cord hemisection in adult guinea pig and injecting differently colored fluorescent labels rostral and caudal to the lesion site. In sham-treated controls, there was much retrograde degeneration of labeled ascending and descending axons 100–300 μm from the transection plane by 60 days postinjury. In animals exposed to oscillating DC EF stimulation however, labeled ascending and descending axons projected to the plane of transection, and in a few cases, fibers were traced around or through the lesion (13). Oscillating EF stimulation protocols have been used also in dogs with a variety of spinal cord injuries (27, 28). In animals with complete paraplegia, there was a statistically improved recovery of a range of neurological behavioral tests and in some cases the restoration of walking. The differences between the sham-treated and the EF-exposed animals were significant therefore, and although some EF-exposed animals might have shown improvement in some functions spontaneously, EF stimulation did enhance this. Borgens and colleagues in Indiana (USA) are using this oscillating DC EF stimulation protocol in clinical trials treating patients with spinal cord injuries (14). A phase one clinical trial has been completed. Ten patients tolerated the oscillator implants well and showed robust improvements in a variety of sensory neurologic functions, but there was no additional improvement in motor functions over the standard methylprednisolone treatment (178).

VII. CONCLUSIONS

There is clear evidence that endogenous EFs are present for many hours or days at wounds and in areas of active cell growth and migration during development. There is strong evidence too that these are essential to regulate appropriate cell behaviors during tissue morphogenesis and regeneration. The complex issue of how EFs interact with other molecular and physical regulators of growth and guidance therefore arises. Consider chemotaxis. Chemical diffusion, for example following release of a charged growth factor from a group of cells, is nonvectorial and occurs evenly in all directions. However, when this occurs in the presence of an EF, which is a vector, directionality will be imposed on the chemical gradient. Importantly, physiological EFs establish chemical gradients in vivo. Current exits the prelimb bud region of amphibian embryos and precedes and predicts the point of emergence of the limb bud by several days (1, 25, 170). Injecting fluorescently labeled charged bovine serum albumin into the prelimb bud region, where the flow of current establishes a steady EF of up to 40 mV/mm (173), resulted not in symmetrical diffusion, but in a comet tail-like distribution of the fluorescent probe driven by electrophoresis within the extracellular space (138). It follows that wherever EFs and soluble charged molecules coexist in vivo, the EF will regulate the establishment and the maintenance of the spatial pattern of the resulting chemical gradient.

In addition to establishing chemical gradients within the extracellular space, DC EFs also stimulate secretion of growth factors (VEGF from endothelial cells) (218) and upregulate expression of growth factor receptors (EGFR on corneal epithelial cells) (219). There are interactions too between a physiological EF and extracellular matrix elements. EF-directed movement of corneal epithelial cells is enhanced in cells interacting with fibronectin or laminin substrates (219), and enhanced or inhibited in neuronal growth cones interacting with specific glycosaminoglycan elements of the extracellular matrix (56). Importantly also, the endogenous current of 120 μA/cm^2 that leaves the blastopore in neurulating *Xenopus* embryos shows transient spikes, with peak currents reaching 200 μA/cm^2 for repeated periods of 1–2 min (173). Therefore, EFs within embryos are switching on and off in a spatially and developmentally controlled manner and also undergoing episodic bursts of activity in particular locations. The effects this might have on locally switching on or off cell cycle regulators, or levels of growth factor receptor expression and growth factor secretion are intriguing.

In short, there is vast untapped potential for EF involvement across a broad spectrum of cell biology. EFs certainly coexist with the more familiar players that control multiple cell behaviors, and it is now timely that their physiological roles are explored more thoroughly. Bioelectricity can, and should, be brought back into mainstream physiology. A rich field awaits.

We are grateful for the continuous support of the Wellcome Trust.

Address for reprint requests and other correspondence: C. D. McCaig, School of Medical Sciences, Institute of Medical Sciences, Univ. of Aberdeen, Aberdeen AB25 2ZD, Scotland (E-mail: c.mccaig@abdn.ac.uk).

REFERENCES

1. **Altizer AM, Moriarty LJ, Bell SM, Schreiner CM, Scott WJ, and Borgens RB.** Endogenous electric current is associated with normal development of the vertebrate limb. *Dev Dyn* 221: 391–401, 2001.
2. **Altizer AM, Stewart SG, Albertson BK, and Borgens RB.** Skin flaps inhibit both the current of injury at the amputation surface and regeneration of that limb in newts. *J Exp Zool* 293: 467–477, 2002.
3. **Ambrose EJ, James AM, and Lowick JHB.** Differences between the electrical charge carried by normal and homologous tumour cells. *Nature* 177: 576–577, 1956.
4. **Ancelin M, Chollet-Martin S, Herve MA, Legrand C, El Benna J, and Perrot-Applanat M.** Vascular endothelial growth factor VEGF 189 induces human neutrophil chemotaxis in extravascular tissue via an autocrine amplification mechanism. *Lab Invest* 84: 502–512, 2004.
5. **Anderson JM.** Molecular structure of tight junctions and their role in epithelial transport. *News Physiol Sci* 16: 126–130, 2001.
6. **Aubry L and Firtel R.** Integration of signaling networks that regulate *Dictyostelium* differentiation. *Annu Rev Cell Dev Biol* 15: 469–517, 1999.
7. **Bailly M, Wyckoff J, Bouzahzah B, Hammerman R, Sylvestre V, Cammer M, Pestell R, and Segall JE.** Epidermal growth factor receptor distribution during chemotactic responses. *Mol Biol Cell* 11: 3873–3883, 2000.
8. **Barker AT, Jaffe LF, and Vanable JW Jr.** The glabrous epidermis of cavies contains a powerful battery. *Am J Physiol Regul Integr Comp Physiol* 242: R358–R366, 1982.
9. **Beitch BR, Beitch I, and Zadunaisky JA.** The stimulation of chloride transport by prostaglandins and their interaction with epinephrine, theophylline, and cyclic AMP in the corneal epithelium. *J Membr Biol* 19: 381–396, 1974.
10. **Beuerman RW and Rosza AJ.** Collateral sprouts are replaced by regenerating neurites in the wounded corneal epithelium. *Neurosci Lett* 44: 99–104, 1984.
11. **Beuerman RW and Schimmelpfenning B.** Sensory denervation of the rabbit cornea affects epithelial properties. *Exp Neurol* 69: 196–201, 1980.
12. **Binggeli R and Weinstein RC.** Membrane potentials and sodium channels: hypotheses for growth regulation and cancer formation based on changes in sodium channels and gap junctions. *J Theor Biol* 123: 377–401, 1986.
13. **Borgens RB.** Restoring function to the injured human spinal cord. *Adv Anat Embryol Cell Biol* 171: 1–155, 2003.
14. **Borgens RB.**http://www RB.vet.purdue.edu/cpr/Center for Paralysis Research website, 2003.
15. **Borgens RB.** Electrically-mediated regeneration and guidance of adult mammalian spinal axons into polymeric channels. *Neuroscience* 91: 251–264, 1999.
16. **Borgens RB.** Introduction. In: *Electric Fields in Vertebrate Repair*, edited by Borgens RB, Robinson KR, Vanable JW Jr, and McGinnis ME. New York: Liss, 1989, p. ix-xxii.
17. **Borgens RB, Blight AR, and McGinnis ME.** Behavioral recovery induced by applied electric fields after spinal cord hemisection in guinea pig. *Science* 238: 366–369, 1987.
18. **Borgens RB, Blight AR, and McGinnis ME.** Functional recovery after spinal cord hemisection in guinea pigs: the effects of applied electric fields. *J Comp Neurol* 296: 634–653, 1990.
19. **Borgens RB, Blight AR, and Murphy DJ.** Axonal regeneration in spinal cord injury: a perspective and new technique. *J Comp Neurol* 250: 157–167, 1986.
20. **Borgens RB, Blight AR, and Murphy DJ.** Transected dorsal column axons within the guinea pig spinal cord regenerate in the presence of an applied electric field. *J Comp Neurol* 250: 168–180, 1986.
21. **Borgens RB, Callahan L, and Rouleau MF.** Anatomy of axolotl flank integument during limb bud development with special reference to a transcutaneous current predicting limb formation. *J Exp Zool* 244: 203–214, 1987.
22. **Borgens RB, Jaffe LF, and Cohen MJ.** Large and persistent electrical currents enter the transected lamprey spinal cord. *Proc Natl Acad Sci USA* 77: 1209–1213, 1980.
23. **Borgens RB, Metcalf ME, and Blight AR.** Delayed application of direct current electric fields in experimental spinal cord injuries. *Restor Neurol Neurosci* 162: 1–7, 1993.
24. **Borgens RB, Roederer E, and Cohen MJ.** Enhanced spinal cord regeneration in lamprey by applied electric fields. *Science* 213: 611–617, 1981.
25. **Borgens RB, Rouleau MF, and DeLanney LE.** A steady efflux of ionic current predicts hind limb development in the axolotl. *J Exp Zool* 228: 491–503, 1983.
26. **Borgens RB and Shi R.** Uncoupling histogenesis from morphogenesis in the vertebrate embryo by collapse of the transneural tube potential. *Dev Dyn* 203: 456–467, 1995.
27. **Borgens RB, Toombs JP, Blight AR, McGinnis ME, Bauer MS, Widmer W, and Cook JR Jr.** Effects of applied electrical fields on clinical cases of complete paraplegia in dogs. *Restor Neurol Neurosci* 5: 305–322, 1993.
28. **Borgens RB, Toombs JP, Breur G, Widmer WR, Water D, Harbath AM, March P, and Adams LG.** An imposed oscillating electrical field improves the recovery of function in neurologically complete paraplegic dogs. *J Neurotrauma* 16: 639–657, 1999.
29. **Borgens RB, Vanable JW Jr, and Jaffe LF.** Bioelectricity and regeneration: large currents leave the stumps of regenerating newt limbs. *Proc Natl Acad Sci USA* 74: 4528–4532, 1977.
30. **Brown MJ and Loew LM.** Electric field-directed fibroblast locomotion involves cell surface molecular reorganization and is calcium independent. *J Cell Biol* 127: 117–128, 1994.
31. **Buck MG and Zadunaisky JA.** Stimulation of ion transport by ascorbic acid through inhibition of 3′:5′-cyclic-AMP phosphodiesterase in the corneal epithelium and other tissues. *Biochim Biophys Acta* 389: 251–260, 1975.
32. **Burger PC, Chandler DB, and Klintworth GK.** Corneal neovascularization as studied by scanning electron microscopy of vascular casts. *Lab Invest* 48: 169–180, 1983.
33. **Campbell DS and Holt CE.** Chemotropic responses of retinal growth cones mediated by rapid local protein synthesis and degradation. *Neuron* 32: 1013–1026, 2001.
34. **Candia OA.** Short-circuit current related to active transport of chloride in frog cornea: effects of furosemide and ethacrynic acid. *Biochim Biophys Acta* 298: 1011–1014, 1973.
35. **Chalfie M, Neufeld AH, and Zadunaisky JA.** Action of epinephrine and other cyclic AMP-mediated agents on the chloride transport of the frog cornea. *Invest Ophthalmol* 11: 644–650, 1972.
36. **Chiang M, Robinson KR, and Vanable JW Jr.** Electrical fields in the vicinity of epithelial wounds in the isolated bovine eye. *Exp Eye Res* 54: 999–1003, 1992.
37. **Chung CY, Funamoto S, and Firtel RA.** Signaling pathways controlling cell polarity and chemotaxis. *Trends Biochem Sci* 26: 557–66, 2001.
38. **Clark RAF.** Wound repair. In: *The Molecular and Cellular Biology of Wound Repair* (2nd ed.), edited by Clark RAF. New York: Plenum, 1998, p. 3–50.
39. **Cole RW and Woodruff RI.** Vitellogenic ovarian follicles of *Drosophila* exhibit a charge-dependent distribution of endogenous soluble proteins. *J Insect Physiol* 46: 1239–1248, 2000.
40. **Comer FI and Parent CA.** PI 3-kinases and PTEN: how opposites chemoattract. *Cell* 109: 541–544, 2002.
41. **Copp AJ, Greene ND, and Murdoch JN.** The genetic basis of mammalian neurulation. *Nat Rev Genet* 4: 784–793, 2003.
42. **Cork RJ, McGinnis ME, Tsai J, and Robinson KR.** The growth of PC12 neurites is biased toward the anode. *J Neurobiol* 25: 1609–1616, 1994.

43. **Cotsarelis G, Cheng SZ, Dong G, Sun TT, and Lavker RM.** Existence of slow-cycling limbal epithelial basal cells that can be preferentially stimulated to proliferate: implications on epithelial stem cells. *Cell* 57: 201–209, 1989.
44. **Cuzick J, Holland R, Barth V, Davies R, Faupel M, Fentiman I, Frischbier HJ, LaMarque JL, Merson M, Sacchini V, Vanel D, and Veronesi U.** Electropotential measurements as a new diagnostic modality for breast cancer. *Lancet* 352: 359–363, 1998.
45. **Davenport RW and Kater SB.** Local increases in intracellular calcium elicit local filopodial responses in *Helisoma* neuronal growth cones. *Neuron* 9: 405–416, 1992.
46. **Davenport RW and McCaig CD.** Hippocampal growth cone responses to focally applied electric fields. *J Neurobiol* 24: 89–100, 1993.
47. **Decker RS.** Disassembly of the zonula occludens during neurulation. *Dev Biol* 81: 12–22, 1981.
48. **Devreotes P and Janetopoulos C.** Eukaryotic chemotaxis: distinctions between directional sensing and polarization. *J Biol Chem* 278: 20445–20448, 2003.
49. **Devreotes PN and Zigmond SH.** Chemotaxis in eukaryotic cells: a focus on leukocytes and *Dictyostelium*. *Annu Rev Cell Biol* 4: 649–686, 1988.
50. **Dineur E.** Note sur la sensibilite des leucocytes a l'electricite. *Bull Seances Soc Belge Microsc* 18: 113–118, 1891.
51. **Djamgoz MBA, Mycielska M, Madeja Z, Fraser SP, and Kohorada W.** Directional movement of rat prostate cancer cells in direct-current electric field: involvement of voltage-gated Na^+ channel activity. *J Cell Sci* 114: 2697–2705, 2001.
52. **Dontchev VD and Letourneau PC.** Growth cones integrate signaling from multiple guidance cues. *J Histochem Cytochem* 51: 435–444, 2003.
53. **Eddleman CS, Bittner GD, and Fishman HM.** Barrier permeability at cut axonal ends progressively decreases until an ionic seal is formed. *Biophys J* 79: 1883–1890, 2000.
54. **Edin ML, Howe AK, and Juliano RL.** Inhibition of PKA blocks fibroblast migration in response to growth factors. *Exp Cell Res* 270: 214–222, 2001.
55. **Emanuelsson H and Arlock P.** Intercellular voltage gradient between oocyte and nurse cell in a polychaete. *Exp Cell Res* 161: 558–561, 1985.
56. **Erskine L and McCaig CD.** Integrated interactions between chondroitin sulphate proteoglycans and weak dc electric fields regulate nerve growth cone guidance in vitro. *J Cell Sci* 110: 1957–1965, 1997.
57. **Erskine L and McCaig CD.** Growth cone neurotransmitter receptor activation modulates electric field guided nerve growth. *Dev Biol* 171: 330–339, 1995.
58. **Erskine L, Stewart R, and McCaig CD.** Electric field directed growth and branching of cultured frog nerves: effects of aminoglycosides and polycations. *J Neurobiol* 26: 523–536, 1995.
59. **Faber DS and Korn H.** Electrical field effects: their relevance in central neural networks. *Annu Rev Physiol* 51: 821–865, 1989.
60. **Fang KS, Farboud B, Nuccitelli R, and Isseroff RR.** Migration of human keratinocytes in electric fields requires growth factors and extracellular calcium. *J Invest Dermatol* 111: 751–756, 1998.
61. **Fang KS, Ionides E, Oster G, Nuccitelli R, and Isseroff RR.** Epidermal growth factor receptor relocalization and kinase activity are necessary for directional migration of keratinocytes in DC electric fields. *J Cell Sci* 112: 1967–1978, 1986.
62. **Ferrier J, Ross SM, Kenehisa J, and Aubon JE.** Osteoclasts and osteoblasts migrate in opposite directions in response to a constant electrical field. *J Cell Physiol* 129: 283–288, 1986.
63. **Fishman HM and Bittner GD.** Vesicle-mediated restoration of a plasmalemmal barrier in severed axons. *News Physiol Sci* 18: 115–118, 2003.
64. **Fitzgerald MJT, Folan JC, and O'Brien TM.** The innervation of hyperplastic epidermis in the mouse: a light microscopic study. *J Invest Dermatol* 64: 169–174, 1975.
65. **Foubister LE.** *Signalling Mechanisms Driving Cell Guidance in a Physiological Electric Field* (PhD Thesis). Aberdeen, Scotland: Univ. of Aberdeen, 2003.
66. **Francis JT, Gluckman BJ, and Schiff SJ.** Sensitivity of neurones to weak electric fields. *J Neurosci* 23: 7255–7261, 2003.
67. **Friend J and Thoft RA.** The diabetic cornea. *Int Ophthalmol Clin* 24: 111–123, 1984.
68. **Fu WM, Liou HC, and Chen YH.** Nerve terminal currents induced by autoreception of acetylcholine release. *J Neurosci* 18: 9954–9961, 1998.
69. **Fu WM, Tang YB, and Lee KF.** Turning of nerve growth cones induced by the activation of protein kinase C. *Neuroreport* 8: 2005–2009, 1997.
70. **Geddes LA and Hoff HE.** The discovery of bioelectricity and current electricity. The Galvani-Volta controversy. *IEEE Spectrum* 8: 38–46, 1971.
71. **Gentzkow GD.** Electrical stimulation to heal dermal wounds. *J Dermatol Surg Oncol* 19: 753–758, 1993.
72. **Gerisch G, Albrecht R, Heizer C, Hodgkinson S, and Maniak M.** Chemoattractant-controlled accumulation of coronin at the leading edge of *Dictyostelium* cells monitored using a green fluorescent protein-coronin fusion protein. *Curr Biol* 5: 1280–1285, 1995.
73. **Giugni TD, Brastan DL, and Haigler HT.** Electric field-induced redistribution and post-field relaxation of epidermal growth factor receptors on A431 cells. *J Cell Biol* 104: 1291–1297, 1987.
74. **Gonczy P.** Mechanisms of spindle positioning: focus on flies and worms. *Trends Cell Biol* 12: 332–339, 2002.
75. **Grahn JC, Reilly DA, Nuccitelli R, and Isseroff RR.** Melanocytes do not migrate directionally in physiological DC electric fields. *Wound Rep Reg* 11: 64–70, 2003.
76. **Guirland C, Buck KB, Gibney JA, DiCicco-Bloom E, and Zheng JQ.** Direct cAMP signaling through G-protein-coupled receptors mediates growth cone attraction by pituitary adenylyate cyclase-activated peptide. *J Neurosci* 23: 2274–2283, 2003.
77. **Haydar TF, Ang E Jr, and Rakic P.** Mitotic spindle rotation and mode of cell division in the developing telencephalon. *Proc Natl Acad Sci USA* 100: 2890–2895, 2003.
78. **Hinkle L, McCaig CD, and Robinson KR.** The direction of growth of differentiating neurones and myoblasts from frog embryos in an applied electric field. *J Physiol* 314: 121–135.
79. **Hoff HE.** Galvani and the pre-Galvanian electrophysiologists. *Ann Sci* 1: 157–172, 1936.
80. **Hopker VH, Shewan D, Tessier-Lavigne M, Poo MM, and Holt C.** Growth-cone attraction to netrin-1 is converted to repulsion by laminin-1. *Nature* 401: 69–73, 1999.
81. **Hotary KB and Robinson KR.** Endogenous electrical currents and the resultant voltage gradients in the chick embryo. *Dev Biol* 140: 149–160, 1990.
82. **Hotary KB and Robinson KR.** The neural tube of the *Xenopus* embryo maintains a potential difference across itself. *Dev Brain Res* 59: 65–73, 1991.
83. **Hotary KB and Robinson KR.** Evidence for a role for endogenous electrical fields in chick embryo development. *Development* 114: 985–996, 1992.
84. **Hotary KB and Robinson KR.** Endogenous electrical currents and voltage gradients in *Xenopus* embryos and the consequences of their disruption. *Dev Biol* 166: 789–800, 1994.
85. **Illingworth CM and Barker AT.** Measurement of electrical currents emerging during the regeneration of amputated fingertips in children. *Clin Phys Physiol Meas* 1: 87–89, 1980.
86. **Ingvar S.** Reactions of cells to the electric current in tissue culture. *Proc Soc Exp Biol Med* 17: 198–199, 1920.
87. **Jaffe LA.** Fast block to polyspermy in sea urchin eggs is electrically mediated. *Nature* 261: 68–71, 1976.
88. **Jaffe LF.** Electrical currents through the developing *Fucus* egg. *Proc Natl Acad Sci USA* 56: 1102–1109, 1966.
89. **Jaffe LF.** Electrophoresis along cell membranes. *Nature* 265: 600–602, 1977.
90. **Jaffe LF.** Extracellular current measurements with a vibrating probe. *Trends Neurosci* 8: 517–521, 1985.
91. **Jaffe LF and Nuccitelli R.** An ultrasensitive vibrating probe for measuring steady extracellular currents. *J Cell Biol* 63: 614–628, 1974.
92. **Jaffe LF and Nuccitelli R.** Electrical controls of development. *Annu Rev Biophys Bioeng* 6: 445–476, 1977.

93. **Jaffe LF and Poo MM.** Neurites grow faster towards the cathode than the anode in a steady electric field. *J Exp Zool* 209: 115–128, 1979.
94. **Jaffe LF and Stern CD.** Strong electrical currents leave the primitive streak of the chick embryo. *Science* 206: 569–571, 1979.
95. **Jenkins LS, Duerstock BS, and Borgens RB.** Reduction of the current of injury leaving the amputation inhibits limb regeneration in the red spotted newt. *Dev Biol* 178: 251–262, 1996.
96. **Jin T, Zhang N, Long A, Parent CA, and Devreotes PN.** Localization of the G protein betagamma complex in living cells during chemotaxis. *Science* 287: 1034–1036, 2000.
97. **Kallin A, Demoulin JB, Nishida K, Hirano T, Ronnstrand L, and Heldin CH.** Gab1 contributes to cytoskeletal reorganization and chemotaxis in response to platelet-derived growth factor. *J Biol Chem* 279: 17897–17904, 2004.
98. **Kimmel AR and Parent CA.** The signal to move: *D. discoideum* go orienteering. *Science* 300: 1525–1527, 2003.
99. **Klyce SD.** Transport of Na, Cl, and water by the rabbit corneal epithelium at resting potential. *Am J Physiol* 228: 1446–1452, 1975.
100. **Klyce SD and Marshall WS.** Effects of Ag^+ on ion transport by the corneal epithelium of the rabbit. *J Membr Biol* 66: 133–144, 1982.
101. **Kobayashi H and Mizisin AP.** Nerve growth factor and neurotrophin-3 promote chemotaxis of mouse macrophages in vitro. *Neurosci Lett* 305: 157–160, 2001.
102. **Koefoed-Johnsen V and Ussing HH.** The nature of the frog skin potential. *Acta Physiol Scand* 42: 298–308, 1958.
103. **Kreppel L and Kimmel AR.** Genomic database resources for *Dictyostelium discoideum*. *Nucleic Acids Res* 30: 84–86, 2002.
104. **Landgren E, Klint P, Yokote K, and Claesson-Welsh L.** Fibroblast growth factor receptor-1 mediates chemotaxis independently of direct SH2-domain protein binding. *Oncogene* 17: 283–291, 1998.
105. **Lawson MA and Maxfield FR.** Ca(2+)- and calcineurin-dependent recycling of an integrin to the front of migrating neutrophils. *Nature* 377: 75–79, 1995.
106. **Levin M and Mercola M.** Gap junctions are involved in the early generation of left-right asymmetry. *Dev Biol* 203: 90–105, 1998.
107. **Levin M and Mercola M.** Gap junction-mediated transfer of left-right patterning signals in the early chick blastoderm is upstream of Shh asymmetry in the node. *Development* 126: 4703–4714, 1999.
108. **Levin M, Johnson RL, Stern CD, Kuehn M, and Tabin C.** A molecular pathway determining left-right asymmetry in chick embryogenesis. *Cell* 82: 803–814, 1995.
109. **Levin M, Thorlin T, Robinson KR, Nogi T, and Mercola M.** Asymmetries in H^+/K^+-ATPase and cell membrane potentials comprise a very early step in left-right patterning. *Cell* 111: 77–89, 2002.
110. **Li S, Zhao T, Xin H, Ye LH, Zhang X, Tanaka H, Nakamura A, and Kohama K.** Nicotinic acetylcholine receptor alpha7 subunit mediates migration of vascular smooth muscle cells toward nicotine. *J Pharmacol Sci* 94: 334–338, 2004.
111. **Li Z, Jiang H, Xie W, Zhang Z, Smrcka AV, and Wu D.** Roles of PLC-beta2 and -beta3 and PI3Kgamma in chemoattractant-mediated signal transduction. *Science* 287: 1046–1049, 2000.
112. **Liu Y, Stein E, Oliver T, Li Y, Brunken WJ, Koch M, Tessier-Lavigne M, and Hogan BL.** Novel role for Netrins in regulating epithelial behavior during lung branching morphogenesis. *Curr Biol* 14: 897–905, 2004.
113. **Lohof AM, Ip Ny, and Poo MM.** Potentiation of developing neuromuscular synapses by the neurotrophins NT-3 and BDNF. *Nature* 363: 350–353, 1993.
114. **Lohof AM, Quillan M, Dan Y, and Poo MM.** Asymmetric modulation of cytosolic cAMP activity induces growth cone turning. *J Neurosci* 12: 1253–1261, 1992.
115. **Marsh G and Beams HW.** In vitro control of growing chick nerve fibers by applied electric currents. *J Cell Comp Physiol* 27: 139–157, 1946.
116. **Mathias RT, Rae JL, and Baldo GJ.** Physiological properties of the normal lens. *Physiol Rev* 77: 21–50, 1997.
117. **Matsuda H, Koyama H, Sato H, Sawada J, Itakura A, Tanaka A, Matsumoto M, Konno K, Ushio H, and Matsuda K.** Role of nerve growth factor in cutaneous wound healing: accelerating effects in normal and healing-impaired diabetic mice. *J Exp Med* 187: 297–306, 1998.
118. **McAvoy JW and Chamberlain CG.** Fibroblast growth factor (FGF) induces different responses in lens epithelial cells depending on its concentration. *Development* 107: 221–228, 1989.
119. **McCaig CD.** Dynamic aspects of amphibian neurite growth and the effects of an applied electric field. *J Physiol* 375: 55–69, 1986.
120. **McCaig CD.** Nerve guidance: a role for bioelectric fields? *Prog Neurobiol* 30: 449–468, 1988.
121. **McCaig CD.** Spinal neurite reabsorption and regrowth in vitro depend on the polarity of an applied electric field. *Development* 100: 31–41, 1987.
122. **McCaig CD.** Nerve growth in the absence of growth cone filopodia and the effects of a small applied electric field. *J Cell Sci* 93: 715–721, 1989.
123. **McCaig CD.** Studies on the mechanism of embryonic frog nerve orientation in a small applied electric field. *J Cell Sci* 93: 722–730, 1989.
124. **McCaig CD.** Nerve growth in a small electric field, and the effects of pharmacological agents on rate and orientation. *J Cell Sci* 95: 617–622, 1990.
125. **McCaig CD.** Nerve branching is induced and oriented by a small applied electric field. *J Cell Sci* 95: 605–615, 1990.
126. **McCaig CD, Allan DW, Erskine L, Rajnicek AM, and Stewart R.** Growing nerves in an electric field. *Neuroprotocols: Companion Methods Neurosci* 4: 134–141, 1994.
127. **McCaig CD and Dover PJ.** Factors influencing perpendicular elongation of embryonic frog muscle cells in a small applied electric field. *J Cell Sci* 98: 497–506, 1991.
128. **McCaig CD and Erskine L.** Nerve growth and nerve guidance in a physiological electric field. In: *Nerve Growth and Guidance*, edited by McCaig CD. London: Portland, 1996, p. 151–170.
129. **McCaig CD and Rajnicek AM.** Electric fields, nerve growth and nerve regeneration. *Exp Physiol* 76: 473–494, 1991.
130. **McCaig CD, Rajnicek AM, Song B, and Zhao M.** Has electrical growth cone guidance found its potential? *Trends Neurosci* 25: 354–359, 2002.
131. **McCaig CD and Robinson KR.** The ontogeny of the transepidermal potential difference in frog embryos. *Dev Biol* 90: 335–339, 1981.
132. **McCaig CD, Sangster L, and Stewart R.** Neurotrophins enhance electric field-directed growth cone guidance and directed nerve branching. *Dev Dyn* 217: 299–308, 2000.
133. **McGinnis ME and Vanable JW Jr.** Wound epithelium resistance controls stump currents. *Dev Biol* 116: 174–183, 1986.
134. **McGinnis ME and Vanable JW Jr.** Electrical fields in *Notophthalmus viridescens* limb stumps. *Dev Biol* 116: 184–193, 1986.
135. **McLaughlin S and Poo MM.** The role of electroosmosis in the electric field-induced movement of charged macromolecules on the surfaces of cells. *Biophys J* 34: 85–93, 1981.
136. **Meili Menu ER, Kooijman R, Van Valckenborgh E, Asosingh K, Bakkus M, Van Camp B, and Vanderkerken K.** Specific roles for the PI3K and the MEK-ERK pathway in IGF-1-stimulated chemotaxis, VEGF secretion and proliferation of multiple myeloma cells: study in the 5T33MM model. *Br J Cancer* 90: 1076–1083, 2004.
137. **Menu E, Kooijman R, Van Valckenborgh E, Asosingh K, Bakkus M, Van Camp B, and Vanderkerken K.** Specific roles for the PI3K and the MEK-ERK pathway in IGF-1-stimulated chemotaxis, VEGF secretion and proliferation of multiple myeloma cells: study in the 5T33MM model. *Br J Cancer* 90: 1076–1083, 2004.
138. **Messerli M and Robinson KR.** Endogenous electrical fields affect the distribution of extracellular protein in *Xenopus* embryos. *Mol Biol Cell* 8: 1296A, 1997.
139. **Metcalf MEM and Borgens RB.** Weak applied voltages interfere with amphibian morphogenesis and pattern. *J Exp Zool* 268: 322–338, 1994.
140. **Ming G, Song H, Berninger B, Inagaki N, Tessier-Lavigne M, and Poo M.** Phospholipase C-gamma and phosphoinositide 3-kinase mediate cytoplasmic signaling in nerve growth cone guidance. *Neuron* 23: 139–148, 1999.
141. **Ming GL, Henley J, Tessier-Lavigne M, Song HJ, and Poo MM.** Electrical activity modulates growth cone guidance by diffusible factors. *Neuron* 29: 441–452, 2001.

142. **Ming GL, Wong ST, Henley J, Yuan XB, Spitzer NC, and Poo MM.** Adaptation in the chemotactic guidance of nerve growth cones. *Nature* 417: 411–418, 2002.
143. **Mir LM, Bureau MF, Gehl J, Rangara R, Rouy D, Caillaud JM, Delaere P, Branellec D, Schwartz B, and Scherman D.** High-efficiency gene transfer into skeletal muscle mediated by electric pulses. *Proc Natl Acad Sci USA* 96: 4262–4267, 1999.
144. **Mycielska ME and Djamgoz MBA.** Cellular mechanisms of direct-current electric field effects: galvanotaxis and metastatic disease *J. Cell Sci* 117: 1631–1639, 2004.
145. **Nakai Y and Kamiguchi H.** Migration of nerve growth cones requires detergent-resistant membranes in a spatially defined and substrate-dependent manner. *J Cell Biol* 159: 1097–1108, 2003.
146. **Nebl T and Fisher PR.** Intracellular Ca^{2+} signals in *Dictyostelium* chemotaxis are mediated exclusively by Ca^{2+} influx. *J Cell Sci* 110: 2845–2853, 1997.
147. **Nguyen QT, Sanes JR, and Lichtman JW.** Pre-existing pathways promote precise projection patterns. *Nature Neurosci* 5: 861–867, 2002.
148. **Nordenstrom BEW.** Electrochemical treatment of cancer. 1. Variable response to anodic and cathodic fields. *Am J Clin Oncol* 12: 530–536, 1989.
149. **Nuccitelli R.** A role for endogenous electric fields in wound healing. In: *Current Topics in Developmental Biology*, edited by Schatten ED. San Diego, CA: Academic, 2004, vol. 58, p. 1–26.
150. **Nuccitelli R, Smart T, and Ferguson J.** Protein kinases are required for embryonic neural crest cell galvanotaxis. *Cell Motil Cytoskeleton* 24: 54–66, 1993.
151. **O'Connor KL, Shaw LM, and Mercurio AM.** Release of cAMP gating by the alpha6beta4 integrin stimulates lamellae formation and the chemotactic migration of invasive carcinoma cells. *J Cell Biol* 143: 1749–1760, 1998.
152. **Onuma EK and Hui SW.** Electric field-directed cell shape changes, displacement, and cytoskeletal reorganization are calcium dependent. *J Cell Biol* 106: 2067–2075, 1988.
153. **Palmer AM, Messerli MA, and Robinson KR.** Neuronal galvanotropism is independent of external Ca^{2+} entry or internal Ca^{2+} gradients. *J Neurobiol* 45: 30–38, 2000.
154. **Parent CA and Devreotes PN.** A cell's sense of direction. *Science* 284: 765–770, 1999.
155. **Partida-Sanchez S, Cockayne DA, Monard S, Jacobson EL, Oppenheimer N, Garvy B, Kusser K, Goodrich S, Howard M, Harmsen A, Randall TD, and Lund FE.** Cyclic ADP-ribose production by CD38 regulates intracellular calcium release, extracellular calcium influx and chemotaxis in neutrophils and is required for bacterial clearance in vivo. *Nat Med* 11: 1209–1216, 2001.
156. **Patel N and Poo MM.** Orientation of neurite growth by extracellular electric fields. *J Neurosci* 2: 483–496, 1982.
157. **Patel NB and Poo MM.** Perturbation of the direction of neurite growth by pulsed and focal electric fields. *J Neurosci* 4: 2939–2947, 1984.
158. **Perrins R and Roberts A.** Nicotinic and muscarinic Ach receptors in rhythmically active spinal neurones in the *Xenopus laevis* embryo. *J Physiol* 478: 221–228, 1994.
159. **Piccolino M.** Luigi Galvani and animal electricity: two centuries after the foundation of electrophysiology. *Brain Res Bull* 46: 381–407, 1997.
160. **Piccolino M.** The bicentennial of the Voltaic battery (1800–2000): the artificial electric organ. *Trends Neurosci* 23: 147–151, 2000.
161. **Pierini LM and Maxfield FR.** Flotillas of lipid rafts fore and aft. *Proc Natl Acad Sci USA* 98: 9471–9473, 2001.
162. **Poo MM.** In situ electrophoresis of membrane components. *Annu Rev Biophys Bioeng* 10: 245–276, 1981.
163. **Poo MM and Robinson KR.** Electrophoresis of concanavalin A receptors in the embryonic muscle cell membrane. *Nature* 265: 602–605, 1977.
164. **Pullar CE, Isseroff RR, and Nuccitelli R.** Cyclic AMP-dependent protein kinase A plays a role in the directed migration of human keratinocytes in a DC electric field. *Cell Motil Cytoskeleton* 50: 207–217, 2001.
165. **Rajnicek AM, Ireland J, Smith LE, and McCaig CD.** Actin microfilaments and microtubules are required for *Xenopus* growth cone turning in a physiological electric field. *J Physiol* 528P: 78P, 2000.
166. **Rajnicek AM and McCaig CD.** cAMP and protein kinase A signaling underlie growth cone turning in a physiological electric field. *Soc Neurosci Abstr* 27: 795.19, 2001.
167. **Rajnicek AM, Robinson KR, and McCaig CD.** The direction of neurite growth in a weak dc electric field depends on the substratum contributions of substrate adhesivity and surface charge. *Dev Biol* 203: 412–423, 1998.
168. **Rajnicek AM, Stump R, and Robinson KR.** An endogenous sodium current may mediate wound healing in *Xenopus* neurulae. *Dev Biol* 128: 290–299, 1988.
169. **Rickert P, Weiner OD, Wang F, Bourne HR, and Servant G.** Leukocytes navigate by compass: roles of PI3Kgamma and its lipid products. *Trends Cell Biol* 10: 466–473, 2000.
170. **Robinson KR.** Endogenous electrical current leaves the limb and pre-limb region of the *Xenopus* embryo. *Dev Biol* 97: 203–211, 1983.
171. **Robinson KR.** The responses of cells to electrical fields: a review. *J Cell Biol* 101: 2023–2027, 1985.
172. **Robinson KR and Messerli MA.** Left/right, up/down: the role of endogenous electrical fields as directional signals in development, repair and invasion. *Bioessays* 25: 759–766, 2003.
173. **Robinson KR and Messerli MA.** Electric embryos: the embryonic epithelium as a generator of developmental information. In: *Nerve Growth and Nerve Guidance*, edited by McCaig CD. London: Portland, 1996.
174. **Robinson KR and Patterson JW.** Localisation of steady currents in the lens. *Curr Eye Res* 2: 843–847, 1982.
175. **Rosza AJ, Guss RB, and Beuerman RW.** Neural remodelling following experimental surgery of the rabbit cornea. *Invest Ophthalmol Vis Sci* 24: 1033–1051, 1983.
176. **Servant G, Weiner OD, Herzmark P, Balla T, Sedat JW, and Bourne HR.** Polarization of chemoattractant receptor signaling during neutrophil chemotaxis. *Science* 287: 1037–1040, 2000.
177. **Servant G, Weiner OD, Neptune ER, Sedat JW, and Bourne HR.** Dynamics of a chemoattractant receptor in living neutrophils during chemotaxis. *Mol Biol Cell* 10: 1163–1178, 1999.
178. **Shapiro S, Borgens RB, Pascuzzi R, Roos K, Groff M, Purvines S, Rodgers RB, Hagy S, and Nelson P.** Oscillating field stimulation for complete spinal cord injury in humans: a Phase 1 trial. *J Neurosurg Spine* 2: 3–10, 2005.
179. **Shi R and Borgens RB.** Embryonic neuroepithelium sodium transport, the resulting physiological potential, and cranial development. *Dev Biol* 165: 105–116, 1994.
180. **Shi R and Borgens RB.** Three dimensional gradients of voltage during development of the nervous system as invisible coordinates for the establishment of the embryonic pattern. *Dev Dynamics* 202: 101–114, 1995.
181. **Siddiqui RA, Akard LP, Garcia JG, Cui Y, and English D.** Chemotactic migration triggers IL-8 generation in neutrophilic leukocytes. *J Immunol* 162: 1077–1083, 1999.
182. **Sillman AL, Quang DM, Farboud B, Fang KS, Isseroff RR, and Nuccitelli R.** Human dermal fibroblasts do not exhibit directional migration on collagen 1 in direct-current electric fields of physiological strength. *Exp Dermatol* 12: 396–402, 2003.
183. **Singleton K and Woodruff RI.** The osmolarity of adult *Drosophila* hemolymph and its effect on oocyte-nurse cell electrical polarity. *Dev Biol* 161: 154–167, 1994.
184. **Song B, Zhao M, Forrester JV, and McCaig CD.** Electrical cues regulate the orientation and frequency of cell division and the rate of wound healing in vivo. *Proc Natl Acad Sci USA* 99: 13577–13582, 2002.
185. **Song B, Zhao M, Forrester JV, and McCaig CD.** Nerves are guided and nerve sprouting is stimulated by a naturally occurring electrical field in vivo. *J Cell Sci* 117: 4681–4690, 2004.
186. **Song HJ and Poo MM.** Signal transduction underlying growth cone guidance by diffusible factors. *Curr Opin Neurobiol* 9: 355–363, 1999.
187. **Song HJ and Poo MM.** The cell biology of neuronal navigation. *Nature Cell Biol* 3: E81–E88, 2001.
188. **Song HJ, Ming GL, and Poo MM.** cAMP-induced switching in turning direction of nerve growth cones. *Nature* 388: 275–279, 1997.

189. **Soong HK, Parkinson WC, Bafna S, Sulik GL, and Huang SCM.** Movements of cultured corneal epithelial cells and stromal fibroblasts in electric fields. *Invest Ophthalmol Vis Sci* 31: 2278–2282, 1990.
190. **Srinivasan S, Wang F, Glavas S, Ott A, Hofmann F, Aktories K, Kalman D, and Bourne HR.** Rac and Cdc42 play distinct roles in regulating PI(3,4,5)P3 and polarity during neutrophil chemotaxis. *J Cell Biol* 160: 375–385, 2003.
191. **Sta Iglesia DD and Vanable JW Jr.** Endogenous lateral electric fields around bovine corneal lesions are necessary for and can enhance normal rates of wound healing. *Wound Rep Reg* 6: 531–542, 1998.
192. **Stewart R, Erskine L, and McCaig CD.** Calcium channel subtypes and intracellular calcium stores modulate electric field stimulated and oriented nerve growth. *Dev Biol* 171: 340–351, 1995.
193. **Stollberg J and Fraser S.** Acetylcholine receptors and concanavalin A-binding sites on cultured *Xenopus* muscle cells: electrophoresis, diffusion and aggregation. *J Cell Biol* 107: 1397–1408, 1988.
194. **Su YA and Poo MM.** Evoked release of acetylcholine from the growing embryonic neuron. *Proc Natl Acad Sci USA* 84: 2540–2544, 1987.
195. **Theis E and Davenport RW.** Independent roles of Rho-GTPases in growth cone and axonal behavior. *J Neurobiol* 54: 358–369, 2003.
196. **Trollinger DR, Isseroff RR, and Nuccitelli R.** Calcium channel blockers inhibit galvanotaxis in human keratinocytes. *J Cell Physiol* 193: 1–9, 2002.
197. **Vanable JW Jr.** Integumentary potentials and wound healing. In: *Electric Fields in Vertebrate Repair*, edited by Borgens RB, Robinson KR, Vanable JW Jr, and McGinnis ME. New York: Liss, 1989, p. 171–224.
198. **Vanable JW Jr.** A history of bioelectricity in development and regeneration. In: *A History of Regeneration Research*, edited by Dinsmore CE. Cambridge, UK: CUP, 1991, p. 151–177.
199. **Van Haastert PJ and Kuwayama H.** cGMP as second messenger during *Dictyostelium* chemotaxis. *FEBS Lett* 410: 25–28, 1997.
200. **Vastrik I, Eickholt BJ, Walsh FS, Ridley A, and Doherty P.** Sema3A-induced growth-cone collapse is mediated by Rac1 amino acids 17–32. *Curr Biol* 9: 991–998, 1999.
201. **Wang E.** *Directed Migration, Re-Orientation and Inhibited Proliferation of Lens Epithelial Cells in Applied Electric Fields* (PhD thesis). Aberdeen, Scotland: Univ. of Aberdeen, 2001.
202. **Wang E, Yin Y, Zhao M, Forrester JV, and McCaig CD.** Physiological electric fields inhibit proliferation of vascular endothelial cells by block at G1. *FASEB J* 17: 458–460, 2003.
203. **Wang E, Zhao M, Forrester JV, and McCaig CD.** Electric fields and MAP kinase signaling regulate early wound healing in lens epithelium. *Invest Ophthalmol Vis Sci* 44: 244–249, 2003.
204. **Wang E, Zhao M, Forrester JV, and McCaig CD.** Re-orientation and faster, directed migration of lens epithelial cells in a physiological electric field. *Exp Eye Res* 71: 91–98, 2000.
205. **Wang E, Zhao M, Forrester JV, and McCaig CD.** Bi-directional migration of lens epithelial cells in a physiological electrical field. *Exp Eye Res* 76: 29–37, 2003.
206. **Webber CA, Hyakutake MT, and McFarlane S.** Fibroblast growth factors redirect retinal axons in vitro and in vivo. *Dev Biol* 236: 24–34, 2003.
207. **Weiner OD, Neilsen PO, Prestwich GD, Kirschner MW, Cantley LC, and Bourne HR.** A PtdInsP(3)- and Rho GTPase-mediated positive feedback loop regulates neutrophil polarity. *Nat Cell Biol* 4: 509–513, 2002.
208. **Weiner OD, Servant G, Welch MD, Mitchison TJ, Sedat JW, and Bourne HR.** Spatial control of actin polymerization during neutrophil chemotaxis. *Nature Cell Biol* 1: 75–81, 1999.
209. **Woodruff RI, Kulp JH, and Lagaccia ED.** Electrically mediated protein movement in *Drosophila* follicles. *Rouxs Arch Dev Biol* 197: 231–238, 1988.
210. **Woodruff RI and Telfer WH.** Polarized intracellular bridges in ovarian follicles of the Cecropia moth. *J Cell Biol* 58: 172–188, 1973.
211. **Wu D, Huang CK, and Jiang H.** Roles of phospholipid signaling in chemoattractant-induced responses. *J Cell Sci* 113: 2935–2940, 2000.
212. **Xiang Y, Li Y, Zhang Z, Cui K, Wang S, Yuan XB, Wu CP, Poo MM, and Duan S.** Nerve growth cone guidance mediated by G-protein coupled receptors. *Nat Neurosci* 5: 843–848, 2002.
213. **Xu J, Wang F, Van Keymeulen A, Herzmark P, Straight A, Kelly K, Takuwa Y, Sugimoto N, Mitchison T, and Bourne HR.** Divergent signals and cytoskeletal assemblies regulate self-organizing polarity in neutrophils. *Cell* 114: 201–214, 2003.
214. **Young SH and Poo MM.** Spontaneous release of transmitter from growth cones of embryonic neurones. *Nature* 305: 634–637, 1983.
215. **Young SH, McLoskey M, and Poo MM.** Migration of cell surface receptors induced by extracellular electric fields: theory and applications. In: *Receptors*. New York: Academic, 1984, vol. 1.
216. **Yuan XB, Jin M, Xu X, Song YQ, Wu CP, Poo MM, and Duan S.** Signalling and crosstalk of Rho GTPases in mediating axon guidance. *Nat Cell Biol* 5: 38–45, 2003.
217. **Zhao M, Agius-Fernandez A, Forrester JV, and McCaig CD.** Orientation and directed migration of cultured corneal epithelial cells in small electric fields are serum dependent. *J Cell Sci* 109: 1405–1414, 1996.
218. **Zhao M, Bai H, Wang E, Forrester JV, and McCaig CD.** Electrical stimulation directly induces pre-angiogenic responses in vascular endothelial cells by signaling through VEGF receptors. *J Cell Sci* 117: 397–405, 2003.
219. **Zhao M, Dick A, Forrester JV, and McCaig CD.** Electric field-directed cell motility involves up-regulated expression and asymmetric redistribution of the epidermal growth factor receptors and is enhanced by fibronectin and by laminin. *Mol Biol Cell* 10: 1259–1276, 1999.
220. **Zhao M, Forrester JV, and McCaig CD.** Physiological electric fields orient the axis of cell division. *Proc Natl Acad Sci* 96: 4942–4946, 1999.
221. **Zhao M, Jin T, McCaig CD, Forrester JV, and Devreotes PN.** Genetic analysis of the role of G protein-coupled receptor signaling in electrotaxis. *J Cell Biol* 157: 921–927, 2002.
222. **Zhao M, Pu J, Forrester JV, and McCaig CD.** Membrane lipids, EGF receptors and intracellular signals co-localize and are polarized in epithelial cells moving directionally in a physiological electric field. *FASEB J* 16: 857–859 and 10.1096/fj.01–0811fje (2002).
223. **Zhao M, Song B, Pu J, Forrester JV, and McCaig CD.** Direct visualization of stratified epithelium reveals that wounds heal by unified sliding of cell sheets. *FASEB J* 17: 397–406, 2003.
224. **Zheng JQ, Felder M, Connor JA, and Poo MM.** Turning of nerve growth cones induced by neurotransmitters. *Nature* 368: 140–144, 1994.
225. **Zheng JQ, Wan JJ, and Poo MM.** Essential role of filopodia in chemotropic turning of nerve growth cone induced by a glutamate gradient. *J Neurosci* 16: 1140–1149, 1996.
226. **Zieske JD, Takahashi H, Hutcheon AEK, and Dalbone AC.** Activation of epidermal growth factor receptor during corneal epithelial cell migration. *Invest Ophthalmol Vis Sci* 41: 1346–1355, 2000.
227. **Zigmond SH.** Signal transduction and actin filament organization. *Curr Opin Cell Biol* 8: 66–73, 1996.
228. **Zwilling E.** The embryogeny of a recessive rumpless condition in chick embryos. *J Exp Zool* 99: 79–91, 1945.